A Study of Hawking Radiation Emission: The Information Paradox and Dark Matter Production from Primordial Black Holes

Evelyn-Andreea Ester

Supervisors: Dr. Daniel Bedingham and Dr. Stephen West

June 11, 2021

Abstract

The black hole information paradox means that an initially pure state irreversibly evolves through Hawking radiation into a thermal mixed state, in contradiction with quantum mechanics unitarity. This paper presents a resolution to this paradox in the context of modified quantum theories involving the spontaneous reduction of the quantum state, originally addressed to solve the quantum measurement problem. An analysis of the entanglement entropy of a collapsed pair within this framework shows that Hawking radiation is indeed a mixed thermal state. Additionally, a dark matter production mechanism via Hawking radiation is analyzed numerically, by considering the decay of an initial distribution of primordial black holes.

ROYAL HOLLOWAY UNIVERSITY OF LONDON

Contents

Acknowledgements

Undertaking this Master's degree has been a truly life-changing experience for me and it would not have been possible without the support and guidance that I received from many people.

Firstly, I would like to express my sincere gratitude to my advisor, Dr Stephen West, for his continuous support through the struggle of learning physics and for being a role model for my future teaching/research career. His unwavering support and belief in me motivated my work towards completing this degree and inspired me to continue my journey to understand how the Universe works. I could not have imagined having a better advisor and mentor for my MSc study.

I would also like to thank Dr Daniel Bedingham for his very insightful comments and suggestions, which are undoubtedly influential in shaping the present work. His guidance provided me with the tools that I needed to choose the right direction and successfully complete this research project.

Of course, none of this would have been possible if it were not for my mother and father and my supportive friends. A very special thank you goes to Sudi, Marina, Srinidhi, Caitlin and Sarah.

Per aspera ad astra.

1 Introduction

The universality of gravity, as expressed by the equivalence principle, allows nature to produce a very strong gravitational field; so strong that it continues to grow up to extreme situations without being counterbalanced by other forces. Such a field can become so strong that it substantially modifies the causal structure of spacetime and produces a region where light is trapped and no particle can escape to infinity.

Quantum mechanics, on the other hand, seems to partially prevent this extreme situation. Black holes are not as "black" as general relativity predicts, but radiate thermally all types of existing quanta. Although an initially small effect, this will make a black hole shrink to a Planck scale, and eventually the black hole will dissappear. This astonishing result has been obtained by Hawking (1975), using the approximation that the spacetime background is kept fixed at all times.

However, the fixed background approximation ignores the effects of radiation on the spacetime geometry, i.e. the backreaction effects on the metric. They are significant even before the black hole reaches the Planck scale, when a yet to be discovered quantum gravity theory is expected to control the process. The reason it is hard to go beyond the fixed background approximations is because one needs to solve the semiclassical Einstein equations, therefore one needs to find an explicit expression for the expectation value of the energy-momentum tensor. This quantity, in turn, depends on the quantum state of matter. This is a fundamental problem of quantum field theory in curved spacetime, and only for conformally flat geometries and conformal fields (such as the ones presented in this paper) a solution can be found analytically. The reduction of the gravity-matter system under spherical symmetry leads to an effective two-dimensional theory, allowing one to use conformally flat metrics as a starting point for the analysis.

The type of radiation emitted does not allow one to retrieve information about the star from which the black hole was created. Therefore, when a black hole has completed its evaporation, this information will be lost forever. This is in direct contradiction with the established principles of quantum mechanics. There have been attempts to address this issue on the basis of quantum treatments of gravitation (for further details see Hossenfelder & Smolin, 2010), however none offer a satisfactory resolution. If one views this singularity as a fundamental boundary of spacetime, one can say that the information is either registered on or escapes through that boundary. If one views the singularity as something that will ultimately be explained by an appropriate quantum gravity (QG) theory, then we must also explain how to reconcile the unitarity of quantum mechanics (QM) evolution with the thermal nature of Hawking radiation. In this paper, we explore a possible resolution of the paradox, by assuming that QG would eventually replace the singularity, but that quantum theory is modified by treating collapse of a wavefunction as a physical process, occurring spontaneously and independently of observers/measuring devices, and the corresponding modification is such that all the initial information is actually lost.

The quantum state reduction model known as continuous spontaneous localisation (CSL) is a collapse model in which the state of each particle undergoes a random collapse to a state localised in position space. From this law of collapses it follows that quantum wavelike behaviour becomes increasingly unstable for systems of increasing size. The formulation of CSL presented by Bedingham (2010) preserves the symmetries of systems of identical particles and enables a straightforward generalisation to relativistic quantum field theory (RQFT). The divergent behaviour due to point interactions is resolved by smearing out the point interaction with a field mediating the interactions between classical stochastic influences and conventional quantum fields. The mechanism involves nonlinear stochastic modifications to the standard description of unitary state evolution and the introduction of a relativistic field in which a quantized degree of freedom is associated to each point in spacetime. By defining the field within the Tomonaga (1946) picture, in which a state is assigned to any given space-like surface, the Lorentz covariance and frame independence can be preserved, therefore this forms the basis of a relativistic CSL collapse mechanism. Applying this mechanism to the black hole case, this means that the system will evolve from an initially pure state to a state representing the proper thermal state of the radiation.

In the second part of the project, we aim to analyze a gravitational infra-red calculable mechanism for dark matter production, using a primordial density of black holes as the source of both the dark matter (DM) relic abundance and the hot Standard Model (SM) plasma. We therefore test the Hawking decay mechanism and calculate the emissivity of heavy and light dark matter particles. For both these regimes, we calculate the DM yield as a function of the initial state and DM mass and spin. Assuming the process starts in a primordial black hole (pBH)-matter-dominated universe, we solve for the rate of BH-mass loss and the emission rate of a particle species numerically using the publicly available `Blackhawk` code. We are also interested in the temperature of the SM radiation bath at the end of pBH decay, (i.e. the reheat temperature) and the yield of DM, imposing observational constraints that match a standard Big Bang Nucleosynthesis (BBN) and a currently observed DM density. The above calculations assume that all pBHs have the same mass. By solving the same equations numerically for a distribution of masses and a distribution of spins, we aim to confirm the conclusion that the dark matter yield remains unaffected.

2 Black Hole Particle Creation

General relativity treats time and space in an intrinsically unified way that ensures diffeomorphism invariance. However, when attempting to apply the canonical quantization procedure to general relativity, the diffeomorphism invariance of the theory has some problematic implications. Starting with the Hamiltonian formulation of the classical theory, it can be shown that the canonical quantization procedure leads to a wave functional that depends only on the spatial metric h_{ab}, but it is independent of "time". The problem of time in quantum gravity is connected to the fact that in GR different characterizations of spacetime using different Cauchy hypersurfaces are equivalent, i.e. classically, a spacetime is completely determined by Cauchy data on any given hypersurface. On a quantum level, this implies that the state characterized in terms of h_{ab} should be independent of the hypersurface. Thus, the problem of time is connected to the fact that information does not change from hypersurface to hypersurface. It seems therefore essential for a quantum theory of gravity that the quantum procedure corresponding to the reconstruction of spacetime carried out in the classical theory be independent of the slicing of spacetime or the choice of lapse and shift. In other words, it seems essential that the theory and reconstruction procedure ensure the diffeomorphism invariance of the quantum characterization of spacetime. We restrict the present discussion to the case of a pure gravity theory, since the inclusion of matter fields will not alter the picture fundamentally (Okon & Sudarsky 2014).

Regarding the black hole information loss problem, a semiclassical treatment - a scheme where the gravitational degrees of freedom are treated using a classical spacetime metric, and the matter degrees of freedom are treated using the formalism of quantum field theory in curved spacetimes - means that we can start with an initial pure quantum state characterizing the system at some initial stage, which then evolves into something that at the quantum level can only be described as a highly mixed quantum state; however the standard considerations of quantum mechanics leads one to expect a fully unitary quantum evolution. If we assume that the singularity must eventually be resolved by an appropriate quantum gravity theory (in the sense of replacing it by something controllable within such a theory and not as any kind of essential boundary), then we must explain how to reconcile the unitarity of quantum mechanics - which essentially requires reversibility of quantum processes and thus preservation of information - with the thermal nature of Hawking radiation - which depends only on the external details characterizing the black hole, namely mass, charge and angular momentum (Bedingham et al. 2016). Dealing with this paradox should account for the fact that a pure state must turn into a quantum thermal state corresponding to a proper mixture (rather than an improper one), i.e. as the interior BH region dissapears and the singularity is removed, the state of the field for asymptotic observers at $\mathscr{I}^+$ has to be described by a density matrix representing an ensemble in which every element is in a pure state (which one ignores) and not by a density matrix which results from tracing out degrees of freedom in some spacetime region (Modak et al. 2015).

The situation changes when a dynamical stochastic collapse is introduced in the theory. In this case, the characterization of the situation is continuously being modified due to the random wavefunction collapses. Therefore, the information difference between two hypersurfaces corresponds to collapse events taking place between the two. In this context, there will be no issues with accepting that black holes really lose information; such a theory allows one to view the black hole evaporation process as a consequence of evolution laws that are characterized by non-unitarity and irreversibility. The proposed collapse model solution originally addresses the measurement problem that arises when one wants to consider that everything, including observers, should be treated in a quantum mechanical framework. In this model, the state of each particle undergoes a random collapse to a state localised in position space. Therefore, quantum wavelike behaviour becomes increasingly unstable for systems of increasing size. CSL preserves the symmetries of systems of particles, therefore its formulation in terms of a stochastic differential equation enables one to generalise to RQFT. The divergent QFT behaviour (arising from point interactions between QF operators in the dynamical equations for the state vector) can be bypassed using a relativistic field that mediates the collapse by smearing the interactions while preserving Lorentz covariance and frame independence, as illustrated by Bedingham (2010).

In order to obtain the right evolution for the matter fields presently considered, we will need to modify the standard CSL model to include a coupling that depends on the spacetime curvature, so that its effects become larger in the vicinity of a black hole.

2.1 The CGHS Black Hole

The CGHS Black Hole is a two dimensional model for which we write the action as

$$S = \frac{1}{2\pi} \int d^2x \sqrt{-g} \left[e^{-2\phi}[R + 4(\nabla\phi)^2 + 4\Lambda^2] - \frac{1}{2}(\nabla f)^2 \right], \tag{1}$$

where R=Ricci scalar, ϕ is the dilaton field (part of the gravity sector), Λ= cosmological constant, f=matter field.

Choosing conformal gauge $ds^2 = -e^{2\rho}dx^+dx^-$, we obtain the free field equation,

$$2\partial_+\partial_-(\rho - \phi) = 0. \tag{2}$$

In the Kruskal gauge, we require that $\rho = \phi$, therefore we have

$$\begin{aligned} ds^2 &= -\frac{dx^+dx^-}{-\Lambda^2 x^+x^- - \frac{M}{\Lambda x_0^+}(x^+ - x_0^+)\Theta(x^+ - x_0^+)}, \\ e^{-2\phi} &= -\Lambda^2 x^+x^- \frac{M}{\Lambda x_0^+}(x^+ - x_0^+)\Theta(x^+ - x_0^+), \end{aligned} \tag{3}$$

with a singularity along the line where the denominator vanishes and a horizon at $x^- = -M/\Lambda^3 x_0^+$.

Sending a pulse of f matter into the linear dilaton vacuum produces a black hole; before the pulse, equation (3) is the vacuum and afterwards it is a black hole of mass M. The solution shown in figure (1) corresponds to the null shell of matter collapsing gravitationally

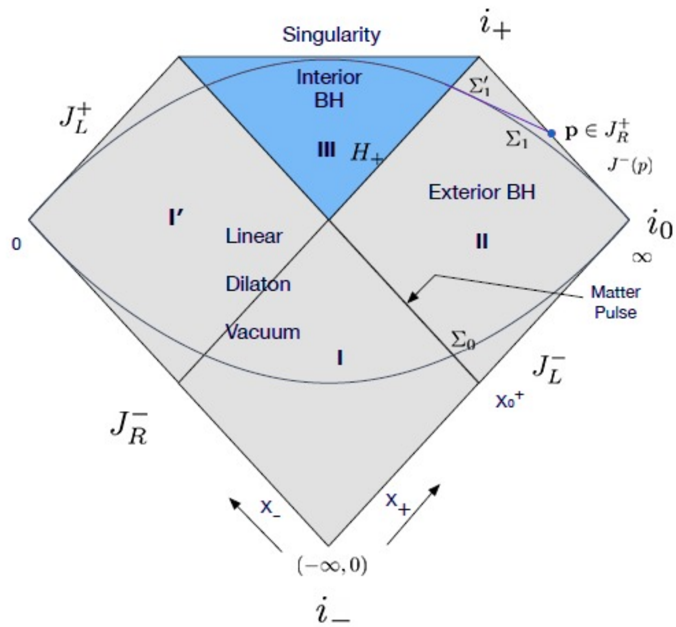

Figure 1: Penrose Diagram for the CGHS Black Hole - adapted from Bedingham et al. (2016).

along the worldline $x^+ = x_0^+$ and forming the black hole. For $x^+ < x_0^+$, i.e. regions I' and I, the solution is the linear dilaton vacuum and has a flat metric,

$$ds^2 = \frac{dx^+ dx^-}{-\Lambda^2 x^+ x^-}, \tag{4}$$

for Kruskal-type coordinates (x^+, x^-). For $x^+ > x_0^+$, i.e. regions II and III, the solution is described by

$$ds^2 = \frac{dx^+ dx^-}{\frac{M}{\Lambda} - \Lambda^2 x^+ (x^- + \Delta)}, \tag{5}$$

which is a black hole with mass M and horizon at $x^- = -\Delta$ (the solution (3) corresponds to $\Delta = M/\Lambda^3 x_0^+$). Unlike $x_0^\pm$, which are constants that can be eliminated by shifts of coordinates, the constant M cannot be removed, and has a clear physical meaning: it corresponds to the mass of the black hole. The $M = 0$ solution is equation (4), for which we can introduce Minkowskian coordinates $\sigma^\pm$, defined by

$$\Lambda x^\pm = \pm e^{\pm \Lambda \sigma^\pm}, \tag{6}$$

so that the metric becomes

$$ds^2 = -d\sigma^+ d\sigma^- = -dt^2 + d\sigma^2, \tag{7}$$

where $\sigma^\pm = t \pm \sigma$, giving the linear form of the dilaton as $\phi = -\Lambda\sigma$. It is also useful to introduce flat coordinates $y^\pm$ for the dilaton vacuum region: these are defined by

$$x^+ = \frac{1}{\Lambda} e^{\Lambda y^+}, \quad x^- = -\Delta e^{-\Lambda y^-}. \tag{8}$$

Thus, the black hole metric is reexpressed as $ds^2 = -dy^+dy^-$ and the horizon is the line $y^- = 0$.

When $M \neq 0$, the higher dimensional solution exhibits both an event horizon and a singularity, and these features are captured by the corresponding two-dimensional near-horizon configuration (5), with scalar curvature

$$R = 8e^{-2\rho}\partial_+\partial_-\rho = \frac{4m\Lambda}{\frac{M}{\Lambda} - \Lambda^2 x^+ x^-}, \tag{9}$$

and curvature singularity at $\Lambda^3 x^+ x^- = M$, as shown in figure (1). The null lines $x^\pm = 0$ correspond to the future and past horizons.

The future event horizon can be seen as the boundary of the past light-cone of future null infinity $\mathscr{I}^+$. An important global feature of the future event horizon is that once it is formed, its generators are null geodesics that never intersect each other and never leave the horizon. This global character requires one to know the entire spacetime geometry for all times before knowing its exact location. This is possible for stationary solutions that describe the geometry after the black hole has settled down and its multipole moments have been radiated away; however at the quantum level, it is an open question to know the spacetime geometry at all times, thus it is very hard to construct the actual event horizon. It is convenient therefore to regard the future event horizon as an apparent horizon, i.e. as the outer boundary of the spacetime region containing trapped surfaces. A trapped surface is a closed spacelike surface such that both the ingoing and outgoing null geodesics orthogonal to it are converging - the physical idea here is that the pull of gravity is so strong that forces the dragging back of light. In our present discussion, the trapped surfaces are given by

$$\partial_+ A \leq 0, \tag{10}$$

where $A = 4\pi r^2$ is the area of the transverse two-sphere. From the four-dimensional solution, we have that

$$\partial_+ A = 8\pi r_0^2 \partial_+ e^{-2\phi}, \tag{11}$$

therefore the boundary of the trapped surfaces is

$$\partial_+ e^{-2\phi} = 0, \tag{12}$$

leading to $x^- = 0$. These coordinates provide the maximal analytical extension of the solution, for which we can choose the Kruskal gauge $\rho = \phi$. The asymptotically flat null coordinates $\sigma^\pm$ are defined as in equation (6), and correspond to the gauge choice

$$\vartheta^\pm = \pm\Lambda\sigma^\pm. \tag{13}$$

Therefore, in the black hole exterior (region II), which is of null Eddington-Finkelstein type, the metric is written as

$$ds^2 = -\frac{dt^2 - d\sigma^2}{(1 + \frac{M}{\Lambda} - \Lambda e^{-\Lambda(\sigma^+ - \sigma^-)})}, \tag{14}$$

with

$$e^{-2\phi} = \frac{M}{\Lambda} + e^{\Lambda(\sigma^+ - \sigma^-)}. \tag{15}$$

In this coordinate system, $\sigma^+ - \sigma^- \to -\infty$ corresponds to the horizon (the surface $\sigma^+ = -\infty$ is the past and $\sigma^- = +\infty$ is the future event horizon). If we now introduce (t, σ) coordinates by $\sigma^\pm = t \pm \sigma$, this is

$$ds^2 = -\frac{dt^2 - d\sigma^2}{(1 + \frac{M}{\Lambda}e^{-2\Lambda\sigma})}, \tag{16}$$

with

$$e^{-2\phi} = -\frac{M}{\Lambda} + e^{2\Lambda\sigma}. \tag{17}$$

Defining the analog of the Schwarzschild gauge as

$$ds^2 = -f(r)dt^2 + \frac{dr^2}{f(r)}, \tag{18}$$

we can use the transformation

$$r = \frac{1}{2\Lambda}\ln(e^{2\Lambda\sigma} + \frac{M}{\Lambda}), \tag{19}$$

such that the resulting metric is

$$ds^2 = -\left(1 - \frac{M}{\Lambda}e^{-2\Lambda r}\right)dt^2 + \frac{dr^2}{(1 - \frac{M}{\Lambda}e^{-2\Lambda r})}. \tag{20}$$

Using the fact that $e^{-2\phi} = e^{2\Lambda r}$, the coordinate system is also valid outside the horizon, which is located at $r_h = \frac{1}{2\Lambda}\ln\frac{M}{\Lambda}$.

2.2 Particle Creation in the CGHS Model

We take the null past asymptotic regions $\mathscr{I}_L^-$ and $\mathscr{I}_R^-$ as the *in* region and the black hole (interior and exterior at $\mathscr{I}^+$) as the asymptotic *out* region; there is no timelike Killing field in the interior region, thus no natural notion of particle or canonical modes in terms of which we quantize the fields, however we shall see that an arbitrary definition can be made. For the quantum treatment of the matter field f, we expand the field operator $\hat{f}$ in the *in* and *out* regions. Therefore, for the *in* region, we have

$$\hat{f}(x) = \sum_\omega (\hat{a}_\omega^R u_\omega^R + \hat{a}_\omega^{R\dagger} u_\omega^{R*} + \hat{a}_\omega^L u_\omega^L + \hat{a}_\omega^{L\dagger} u_\omega^{L\dagger}), \tag{21}$$

where the operators $\hat{a}_\omega^{R/L\dagger}$ are the creation operators appropriate to the *in* region.

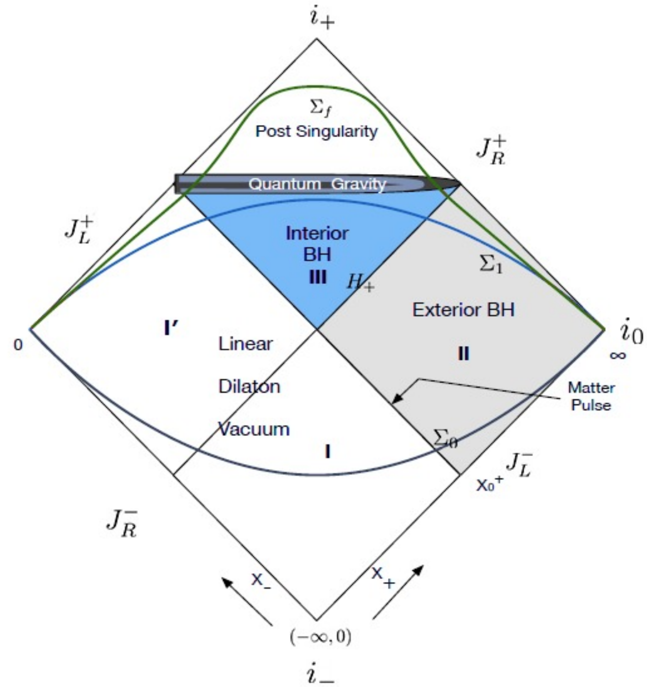

Figure 2: Penrose Diagram for the CGHS Black Hole including the Post-Quantum Gravity Region - adapted from Bedingham et al. (2016).

The basis of modes is given by

$$u_\omega^R = \frac{1}{\sqrt{4\pi\omega}} e^{-i\omega y^-} \tag{22}$$

$$u_\omega^L = \frac{1}{\sqrt{4\pi\omega}} e^{-i\omega y^+}, \tag{23}$$

$$\tag{24}$$

where $\omega > 0$ and the superscripts R/L refer to right and left moving modes, respectively. These modes define an *in* vacuum right $|0\rangle_R^{in}$ and an *in* vacuum left $|0\rangle_L^{in}$, whose tensor product $|0\rangle_R^{in} \otimes |0\rangle_R^{in}$ defines the *in* vacuum.

We now expand the field in the *out* region in a similar manner, by considering the complete set of modes that have support on the outside (region II in figure (2)) and on the inside (region III in figure (2)) of the event horizon. Thus, we have

$$\hat{f}(x) = \sum_\omega (\hat{b}_\omega^R v_\omega^R + \hat{b}_\omega^{R\dagger} v_\omega^{R*} + \hat{b}_\omega^L v_\omega^L + \hat{b}_\omega^{L\dagger} v_\omega^{L*}) + \tag{25}$$

$$+ \sum_{\tilde{\omega}} (\hat{\tilde{b}}_{\tilde{\omega}}^R \tilde{v}_{\tilde{\omega}}^R + \hat{\tilde{b}}_{\tilde{\omega}}^{R\dagger} \tilde{v}_{\tilde{\omega}}^{R*} + \hat{\tilde{b}}_{\tilde{\omega}}^L \tilde{v}_{\tilde{\omega}}^L + \hat{\tilde{b}}_{\tilde{\omega}}^{L\dagger} \tilde{v}_{\tilde{\omega}}^{L*}), \tag{26}$$

where the $\hat{b}_\omega^{R/L\dagger}, \hat{\tilde{b}}_\omega^{R/L\dagger}$ are the creation operators used for the *out* region. Annihilation and creation operators multiply positive and negative frequency modes, respectively. The equations of motion imply the existence of the Klein-Gordon inner product

$$\left(\hat{f}, \hat{g}\right) = -i \int_{\Sigma} d\Sigma^{\mu} \hat{f} \nabla_{\mu} \hat{g}^{*}, \tag{27}$$

for any arbitrary Cauchy surface Σ. We will hereafter consider that the operators with-/without tildes are associated with the interior/exterior black hole regions, respectively. We do not expect the arbitrariness in the basis choice inside the horizon to affect any physical results, since there is no canonical definition of particles there and the quantities of interest will be, in principle, observable by asymptotic observers. The basis of modes in the exterior can be taken as

$$v_{\omega}^{R} = \frac{1}{\sqrt{4\pi\omega}} e^{-i\omega\sigma^{-}} \Theta(-(x^{-} + \Delta)), \tag{28}$$

$$v_{\omega}^{L} = \frac{1}{\sqrt{4\pi\omega}} e^{-i\omega\sigma^{+}} \Theta(x^{+} - x_{0}^{+}). \tag{29}$$

The operators $\hat{a}_{\omega}$ satisfy the usual commutator relations

$$[\hat{a}_{\omega}, \hat{a}_{\omega'}^{\dagger}] = \delta(\omega - \omega'), \quad [\hat{a}_{\omega}, \hat{a}_{\omega'}] = 0, \quad [\hat{a}_{\omega}^{\dagger}, \hat{a}_{\omega'}^{\dagger}] = 0, \tag{30}$$

and similarly for $\hat{b}_{\omega}$ and $\hat{\tilde{b}}_{\omega}$. We also define the *in* and *out* vacua by

$$\hat{a}_{\omega} \left|0\right\rangle_{in} = 0, \quad \hat{b}_{\omega} \left|0\right\rangle_{ext} = 0, \quad \hat{\tilde{b}}_{\omega} \left|0\right\rangle_{int} = 0, \tag{31}$$

for $\omega > 0$; the definition for the internal "vacuum" will not affect the calculation of emission of particles to $\mathscr{I}^{+}$.

Although the *in* and *out* regions are asymptotically flat, their natural timelike coordinates are related such that a field mode with positive frequency according to observers in a region becomes a mixture of positive and negative frequencies according to observers in the other region. This mixing is interpreted as particle creation. Thus, in order to determine the number of particles created by the gravitational field and emitted to infinity, one simply has to calculate the Bogolyubov coefficients $\alpha_{\omega\omega'}$ and $\beta_{\omega\omega'}$ defined below (Hawking, 1975):

$$v_{\omega} = \sum_{\omega'} [\alpha_{\omega\omega'} u_{\omega'} + \beta_{\omega\omega'} u_{\omega'}^{*}]. \tag{32}$$

These are obtained as

$$\alpha_{\omega\omega'} = \frac{1}{2\pi}(v_{\omega}, u_{\omega}'), \quad \beta_{\omega\omega'} = -\frac{1}{2\pi}(v_{\omega}, u_{\omega'}^{*}), \tag{33}$$

and similarly for the internal modes $\tilde{\alpha}_{\omega\omega'}, \tilde{\beta}_{\omega\omega'}$. Equivalence of expansions (21) and (26) gives the relation between the field operators in the *in* and *out* regions,

$$\begin{aligned}
\hat{a}_\omega &= \sum_{\omega'} \left[\hat{b}_{\omega'} \alpha_{\omega'\omega} + \hat{b}^\dagger_{\omega'} \beta^*_{\omega'\omega} + \hat{\tilde{b}}_{\omega'} \hat{\tilde{\alpha}}_{\omega'\omega} + \hat{\tilde{b}}^\dagger_{\omega'} \tilde{\beta}^*_{\omega'\omega} \right], \\
\hat{b}_\omega &= \sum_{\omega'} \left[\alpha^*_{\omega\omega'} \hat{a}_{\omega\omega'} - \beta^*_{\omega\omega'} a^\dagger_{\omega'} \right], \\
\hat{\tilde{b}}_\omega &= \sum_{\omega'} \left[\tilde{\alpha}^*_{\omega\omega'} \hat{a}_{\omega'} - \tilde{\beta}^*_{\omega\omega'} a^\dagger_{\omega'} \right].
\end{aligned} \tag{34}$$

If $\beta_{\omega\omega'} \neq 0$, then the *in* vacuum description is not the same as the *out* vacuum; particle creation has occurred, i.e. if $N^{out}_\omega = \hat{b}^\dagger_\omega \hat{b}_\omega$ is the number operator for modes of frequency ω, then it follows from equation (34) that

$$_{in}\langle 0 | N^{out}_\omega | 0 \rangle_{in} = \sum_{\omega'} |\beta_{\omega\omega'}|^2. \tag{35}$$

For the CGHS model, we calculate the Bogolyubov coefficients using the relation between the coordinates

$$\sigma^- = -\frac{1}{\Lambda} \ln \left[\Lambda\Delta(e^{-\Lambda y^-} - 1) \right], \tag{36}$$

so that

$$v_\omega = \frac{1}{\sqrt{2\omega}} \exp\{ \frac{i\omega}{\Lambda} \ln[\Lambda\Delta(e^{-\Lambda y^-} - 1)] \} \Theta(y^-). \tag{37}$$

Therefore, at the null surface $\mathscr{I}^-$ we compute the inner products given in equation (33) as

$$\begin{aligned}
\alpha_{\omega\omega'} &= -\frac{i}{\pi} \int_{-\infty}^0 dy^- v_\omega \partial_- u^*_{\omega'} \\
&= \frac{1}{2\pi} \sqrt{\frac{\omega'}{\omega}} \int_{-\infty}^0 dy^- \exp\{ \frac{i\omega}{\Lambda} \ln[\Lambda\Delta(e^{-\Lambda y^-} - 1)] + i\omega' y^- \}, \\
\beta_{\omega\omega'} &= \frac{i}{\pi} \int_{-\infty}^0 dy^- v_\omega \partial_- u_{\omega'} \\
&= \frac{1}{2\pi} \sqrt{\frac{\omega'}{\omega}} \int_{-\infty}^0 dy^- \exp\{ \frac{i\omega}{\Lambda} \ln[\Lambda\Delta(e^{-\Lambda y^-} - 1)] - i\omega' y^- \}.
\end{aligned} \tag{38}$$

One can further use the pole prescriptions given in Giddings & Nelson (1992) to check that the expansion (32) holds and that the Bogolyubov coefficients satisfy the completeness identity

$$\sum_{\omega'} \alpha_{\omega\omega'} \alpha^*_{\omega''\omega'} - \beta_{\omega\omega'} \beta^*_{\omega''\omega'} = \delta(\omega - \omega''). \tag{39}$$

Similarly, we use the $\pm y$ coordinates to define the modes in region III, by using the expression for $\sigma^-(y^-)$ from equation (to be defined) and the substitution in the argument y^- by $-y^-$, i.e.

$$\tilde{v}_\omega(y^-) = v^*_\omega(-y^-), \tag{40}$$

which gives

$$\tilde{\alpha}_{\omega\omega'} = \alpha^*_{\omega\omega'}, \quad \tilde{\beta}_{\omega\omega'} = \beta^*_{\omega\omega'}. \tag{41}$$

In conclusion we have obtained two sets of Bogolyubov coefficients for the right moving sector: the first corresponding to the relations between the modes in regions I' and III, and the second between the modes in regions I and II. We are interested in the transformation from the *in* to the *exterior* modes (i.e. regions I and III), because this yields the Hawking flux. Thus, we will obtain the Hawking radiation in the asymptotic limit from the right moving sector and the negative flux at the horizon given by the left moving sector.

The late-time Bogolyubov transformation is found by replacing the integrand value of equation (38) by its approximate value near the horizon, i.e. $y^- = 0$, which gives

$$\alpha_{\omega\omega'} \approx \frac{1}{2\pi}\sqrt{\frac{\omega'}{\omega}} \int_{-\infty}^{0} dy^- \exp\{\frac{i\omega}{\Lambda}\ln(-\Lambda^2\Delta y^-) + i\omega' y^-\}, \tag{42}$$

and similarly for $\beta_{\omega\omega'}$, which differs from this only by the sign of ω' in the integrand. If we now substitute $y^- \to -y^-$, we get the relation

$$\alpha_{\omega\omega'} \approx -e^{\pi\omega/\Lambda}\beta_{\omega\omega'}. \tag{43}$$

Setting $\omega = \omega''$ in the completeness identity (39) gives

$$\sum_{\omega'} |\alpha_{\omega\omega'}|^2 + |\beta_{\omega\omega'}|^2 = t, \tag{44}$$

with $\delta(0)$ replaced by a large time cutoff t, giving the result

$${}_{in}\langle|0N^{out}_\omega|0\rangle_{in} = \sum_{\omega'} |\beta_{\omega\omega'}|^2 \approx t\ \frac{e^{-2\pi\omega/\Lambda}}{1-e^{-2\pi\omega/\Lambda}}, \tag{45}$$

thus the modes are thermally populated at temperature $T_H = \Lambda/2\pi$.

For the present purpose, we omit the issue of backreaction on the metric. It is a fundamental problem of quantum field theory in curved spacetime to find an expression for the expectation value of the stress tensor for matter fields in a curved background. This is an obstacle one faces before considering the backreaction of Hawking radiation on the black hole geometry. As it is indicated by Fabbri & Navarro-Salas (2005), no exact analytical expression is known, even for a fixed Schwarzschild spacetime. However, a solution to the problem exists for conformally flat geometries; for the two-dimensional CGHS model considered by Giddings & Nelson (1992), coupling the stress tensor to gravity will give an accurate representation of the effects of backreaction. These become important when calculating the emitted energy flux (i.e. luminosity $\mathcal{L}$) in section 4.3. In a realistic model, the black hole mass changes, and so does its instantaneous temperature. Moreover, the backreaction effect is what allows us to further consider that the singularity will eventually be replaced by a low-energy state and to expect flat space to emerge on the other side of the QG region (Modak et al. 2015).

2.3 Fock Space Field Quantization

We now use the defined bases of modes to construct the Fock space quantization of the field in each region, using standard methods discussed by Wald (1984) and Mukhanov & Winitzki (2007). We proceed by constructing the space for the right moving sector of the field in the exterior region, $\mathscr{F}^R_{ext}$ for the *in* and *out* regions as

$$\mathscr{F}_{in} = \mathscr{F}^R_{in} \otimes \mathscr{F}^L_{in}, \tag{46}$$

$$\mathscr{F}_{out} = \mathscr{F}^R_{int} \otimes \mathscr{F}^L_{int} \otimes \mathscr{F}^R_{ext} \otimes \mathscr{F}^L_{ext}. \tag{47}$$

We introduce the complete set of orthonormal wavepacket modes,

$$v_{jn} = \epsilon^{-\frac{1}{2}} \int_{j\epsilon}^{(j+1)\epsilon} d\omega \, e^{2\pi i\omega n/\epsilon} v_\omega, \tag{48}$$

with $j, n \in \mathbb{Z}$ and $j \geq 0$. These wavepackets have frequency $\omega \approx \omega_j$, with $\omega_j \approx j\epsilon$ and are peaked about $\sigma^- = 2\pi n/\epsilon$ with width ϵ^{-1}. We consider the distribution of occupation numbers $F = \{..., F_{nj}, ...\}$, with $F_{nj} \in \mathbb{Z}$, such that $\sum_{nj} F_{nj} < \infty$ and the normalized state

$$|F\rangle^R_{ext} = C_F \prod_{nj} (\hat{b}^\dagger_{nj})^{F_{nj}} \, |0\rangle^{ext}_R \,, \tag{49}$$

where C_F is a normalization factor. Then the set of all possible states of this form, $|F\rangle^R_{ext}$ forms a basis for $\mathscr{F}^R_{ext}$. Analogous for the bases of all other Fock spaces. Following Giddings & Nelson (1992), we write the *in* vacuum state as a superposition of all *out* basis particle states. Since non-trivial Bogolyubov coefficients exist only for right-moving modes, we can expand formally $|0\rangle^R_{in}$ in the basis of *out* (*ext* and *int*) right moving sector's Fock space. This is the standard CGHS black hole Hawking radiation derivation, which gives

$$|0\rangle^{in}_R = N \sum_F e^{-\frac{\pi}{\Lambda} E_F} \, |F\rangle^{int}_R \otimes |F\rangle^{ext}_R \,, \tag{50}$$

where N is a normalization factor and $E_F = \sum_{nj} \omega_{nj} F_{nj}$ is the energy of state $|F\rangle^{ext}_R$ with respect to late-time observers near $\mathscr{I}^+$, and $\sum_F \equiv \sum_{F_{nj}} \sum_{F_{n'j'}} ...$ with all sums running from 0 to ∞. Hence, the full vacuum (assuming that the vacuum state for left modes is unchanged due to trivial Bogolyubov coefficients) can be written as

$$\begin{aligned} |0\rangle^{in} &= |0\rangle^{in}_R \otimes |0\rangle^{in}_L \\ &= N \sum_F e^{-\frac{\pi}{\Lambda} E_F} \, |F\rangle^{int}_R \otimes |F\rangle^{ext}_R \otimes |0\rangle^{in}_L \,. \end{aligned} \tag{51}$$

The thermal coefficients appearing later in the density matrix operator ρ^{in}_R (equation 77) come from the explicit Bogolyubov coefficients evaluated in the late-time limit (equation 42), although in the CGHS model they can be evaluated without taking this limit. It is further shown by Giddings & Nelson (1992) that the late-time density matrix is purely thermal (if one neglects the backreaction), thus it has no hidden correlations that would correspond to information escaping from the black hole.

2.4 CSL Collapse Model

A simple form of CSL describes the wavefunction collapse towards one of the eigenstates of an operator $\hat{A}$ at a rate proportional to λ, defined below in equation (71). In order to specify this, we need to consider a stochastically modified version of the Schrödinger equation along with a probability rule. We implement therefore the (relativistically invariant) interaction picture described by Tomonaga (1946) in which the quantum state of matter ψ_Σ is assigned to a spacelike hypersurface Σ. As we advance the hypersurface Σ to the future via a foliation of spacetime, the state changes according to the Tomonaga equation,

$$i\frac{\delta\left|\psi_\Sigma\right\rangle}{\delta\Sigma(x)} = \hat{\mathcal{H}}_{int}(x)\left|\psi_\Sigma\right\rangle, \tag{52}$$

where $\hat{\mathcal{H}}_{int}$ is the interaction Hamiltonian density. The functional derivative is defined as

$$\frac{\delta\left|\psi_\Sigma\right\rangle}{\delta\Sigma(x)} = \lim_{\Sigma'\to\Sigma}\frac{\left|\psi_{\Sigma'}\right\rangle - \left|\psi_\Sigma\right\rangle}{\Delta V}, \tag{53}$$

where ΔV is the invariant spacetime volume enclosed by Σ and Σ' with a partial ordering structure $\Sigma \prec \Sigma'$ (i.e. no point in Σ is to the causal future of any point in Σ'). Covariance requires

$$[\hat{\mathcal{H}}_{int}(x), \hat{\mathcal{H}}_{int}(y)] = 0, \tag{54}$$

for spacelike separated x and y. This guarantees foliation independence of the state development. In the simple case where the Hamiltonian is zero, the general solution of the stochastically modified Schrödinger equation is

$$\left|\psi, t\right\rangle = e^{-\frac{1}{4\lambda t}[B(t)-2\lambda t\hat{A}]^2}\left|\psi, 0\right\rangle, \tag{55}$$

where $B(t)$ is a stochastic function of time and $\hat{A}$ is a Hermitian operator. Assuming that the initial state has unit norm, the probability rule for a specific realization of the function $B(t)$ at time t has the value in the interval $[B(t), B(t)+dB(t)]$ is

$$P[B(t)]dB(t) = \frac{dB(t)}{\sqrt{2\pi\lambda t}}\langle\psi, t|\psi, t\rangle. \tag{56}$$

When including a nontrivial Hamiltonian, the state vector dynamics is easily understood in terms of small individual time steps; in an infinitesimal dt interval, the evolution equation is

$$\left|\psi, t\right\rangle = e^{-dt\left[i\hat{H}+\frac{1}{4\lambda}[w(t)-2\lambda\hat{A}]^2\right]}\left|\psi, t-dt\right\rangle, \tag{57}$$

where $w(t) = dB(t)/dt$ is a random white noise function and $B(t)$ corresponds to the Wiener process appearing in the corresponding Langevin equation in the standard treatment of Brownian motion, as illustrated by Cowan (2005). The probability that its value at t lies within the interval $[w(t), w(t)+dw(t)]$ is now

$$P(w)dw = \frac{\langle\psi, t|\psi, t\rangle}{\langle\psi, t-dt|\psi, t-dt\rangle}\frac{dw(t)}{\sqrt{2\pi\lambda/dt}}. \tag{58}$$

Over a finite time interval, e.g. from $t' = 0$ to t in the step of dt, equation (57) becomes

$$|\psi, t\rangle = \mathscr{T} e^{-\int_0^t dt' \left[i\hat{H} + \frac{1}{4\lambda}[w(t') - 2\lambda \hat{A}^2] \right]} |\psi, 0\rangle \,, \tag{59}$$

where $\mathscr{T}$ is the time-ordering operator. The probability that the function $w(t)$ lies in $Dw(t)$ with the restriction that $w(t_i)$ lies in the interval $[w(t_i), w(t_i) + dw(t_i)]$ is

$$P(w)Dw(t) = \langle\psi, t|\psi, t\rangle \prod_{i=1}^{N} \frac{dw(t_i)}{\sqrt{2\pi\lambda/dt}}, \tag{60}$$

which is a joint probability distribution over $t \in [0, t]$ deduced from equation (58) assuming that the initial state vector was normalized to unity. For later times, the state vector evolves dynamically (i.e. not normalized), so equation (60) says that the state vectors with the largest norm are the most probable - this does not contradict the standard normalization requirement of quantum mechanical theory since probabilities are assigned to the realization of stochastic functions instead of quantum mechanical amplitudes. The total probability for realization of an arbitrary stochastic function is shown to be

$$\int PDw(t) = 1. \tag{61}$$

The CSL dynamics drives an initial state towards one of the eigenstates of the collapse operator $\hat{A}$, due to the presence of the stochastic function $w(t)$. If we consider an ensemble of identically prepared systems and apply the CSL dynamics, the result will be an ensemble of differently evolved state vectors characterized by a different $w(t)$. Using equation (59), the density matrix of an ensemble of evolved vectors is

$$\rho(t) = \mathscr{T} e^{-\int_0^t dt' \left[i(\underset{\rightarrow}{\hat{H}} - \underset{\leftarrow}{\hat{H}}) + \frac{\lambda}{2}(\underset{\rightarrow}{\hat{A}} - \underset{\leftarrow}{\hat{A}})^2 \right]} \rho(0), \tag{62}$$

where the arrows under the operators indicate that the operator acts on the right or on the left of $\rho(0)$, respectively. The resulting evolution equation for the density matrix is

$$\frac{d}{dt}\rho(t) = -i[\hat{H}, \rho(t)] - \frac{\lambda}{2}[\hat{A}, [\hat{A}, \rho(t)]]. \tag{63}$$

2.5 Modified CSL Evolution

Following Modak et al. (2015) and Bedingham et al. (2016), we consider in this section the CSL evolution of states of a real scalar quantum field in the CGHS black hole. Consequently, we work in the interaction picture, where the evolution of the field is encoded in the quantum field operators and the CSL effects are treated as an interaction and embedded in the evolution of the quantum states. We proceed by foliating the spacetime in order to have a well-defined evolution operator connecting the states associated with different specific hypersurfaces. A foliation of spacetime is any maximally ordered chain of surfaces. In a model with no preferred reference frame like the one we are considering in this paper, the foliation should not have any physical significance - it should be the analogous of the choice of gauge.

As described previously, the spacetime metric in the null Kruskal coordinates (x^+, x^-) is given in equations (4) and (5). We introduce the Kruskal coordinates

$$T = \frac{x^+ + x^- + \Delta}{2}, \quad X = \frac{x^+ - x^- - \Delta}{2}. \tag{64}$$

The metric in the black hole region (interior and exterior - regions II and III, respectively) becomes

$$ds^2 = -\frac{dT^2 - dX^2}{\frac{M}{\Lambda} - \Lambda^2(T^2 - X^2)}, \ (-\infty \leq T \leq \infty, -\infty \leq X \leq \infty). \tag{65}$$

We can relate the above coordinates to the Schwarzschild (t, r) coordinates by

$$\tanh(\Lambda t) = \frac{T}{X}, \tag{66}$$

$$-\frac{1}{\Lambda^2}(e^{2\Lambda r} - \frac{M}{\Lambda}) = T^2 - X^2, \tag{67}$$

where the time coordinate is only well-defined in region II, similar to the Schwarzschild case. Using equation (to be defined), we find the Ricci curvature to be

$$R = \frac{4M\Lambda}{\frac{M}{\Lambda} - \Lambda^2(T^2 - X^2)}, \tag{68}$$

therefore the singularity is located at $M/\Lambda = \Lambda^2(T^2 - X^2)$.

We define the foliation Σ_τ and the related coordinates (τ, ζ) covering the regions II and III. The hypersurface Σ_τ is specified to follow in the region III ($e^2\Lambda r < M/\Lambda$) a curve $r = \text{const}$ given by equation (67) and in the region II a line $t = \text{const}$ given by equation (66), connected by a line $T = \text{const}$. A simple smoothing procedure can then be used at the junction points defining the foliation without affecting the essence of the construction. This construction now divides the spacetime into three sectors, corresponding to the black hole interior and exterior, and foliation connector regions, respectively. These evolve forward in time and do not cross each other at any stage. Explicit transformations for $\tau(T, X)$ and $\zeta(T, X)$ were obtained by Modak et al. (2015), thus using the (τ, ζ) parametrization, the Ricci scalar is now

$$R(\tau) = \frac{4M\Lambda}{M/\Lambda - \Lambda^2\tau^2}, \tag{69}$$

and the position of the singularity is given by a finite $\tau_S = \frac{M^{1/2}}{\Lambda^{3/2}}$. We are interested in using the foliation to evolve quantum states with CSL in the open interval $(0, \tau_S)$. The foliation can be continued arbitrarily backwards to cover the rest of the spacetime before the singularity; however the proposed CSL parameter will only become large in the regions of large curvature (the ones covered by the foliation derived above).

The CSL theory is generalized to drive an initial state into a joint eigenstate of a set of mutually commuting operators $\{A^\alpha\}$ - called the set of collapse operators - which requires implementing a noise function w^α for each A^α in this set. In this case, equation (62) becomes

$$\rho(t) = \mathscr{T} e^{-\int_0^t dt' \left[i[\hat{H} - \hat{H}] + \frac{\lambda}{2} \sum_\alpha [A^\alpha - A^\alpha]^2 \right]} \rho(0). \tag{70}$$

In adapting the CSL dynamics to the CGHS scenario, we assume that the theory contains an underlying connection (yet to be experimentally confirmed) between the dynamical collapse of quantum states and gravity. Hence, assuming that the rate of collapse is enhanced by the curvature of the spacetime - a proposal known as the "Weyl curvature hypothesis" and explained in Penrose (2004) - information might be completely destroyed due to the stochastic nature of the process. In order to prove that this holds, one needs to perform experiments or analyze observations of a quantum process in the presence of ultra-strong gravity.
Since the hypersurfaces described by the foliation have a constant R inside the black hole (in almost all the part of Σ_S), we have that, for the region of interest, the rate of collapse λ will be dependent on the Ricci scalar:

$$\lambda(R) = \lambda_0 \left[1 + \left(\frac{R}{\mu} \right)^\gamma \right], \tag{71}$$

where R is the Ricci scalar of the CGHS spacetime and $\mu, \gamma \geq 1$ are constants. Note that for the CGHS model, we have taken the rate of collapse to be dependent on the Ricci scalar instead, because the two-dimensional conformally flat CGHS configuration we are considering has a vanishing Weyl tensor. This choice ensures that the initial state is driven towards the eigenstate of the collapse operators in a finite amount of time τ, such that is we were to continue the evolution up to the singularity (except where quantum gravity effects dominate and the semiclassical picture breaks down), the state of the field would be one of definite particles in each mode with a smooth expectation value for the energy-momentum tensor.

Collapse operators have to be smooth and locally constructed from the quantum fields, therefore we choose the collapse operators to count the number of right moving particles inside the black hole in a definite state, as described by late-time observers at $\mathscr{I}^+$ (i.e. the observers that describe the Hawking radiation). The Fock space of states of the quantum field in the interior black hole region is $\mathscr{F}_R^{int} \otimes \mathscr{F}_L^{int}$ and has the basis $\{|F\rangle_R^{int} \otimes |G\rangle_L^{int}\}$.

The action of the right-moving particles number operator $(N_R^{int})_{nj} = \hat{\tilde{b}}_{nj}^{R\dagger} \hat{\tilde{b}}_{nj}^R$ acting of $\mathscr{F}_R^{int}$ is

$$(N_R^{int})_{nj} \, |F\rangle_R^{int} = F_{nj} \, |F\rangle_R^{int} \, . \tag{72}$$

Then, the proposed set of collapse operators $\{\tilde{N}_{nj}\}$ in the CSL evolution only modifies the black hole interior right moving modes, i.e.

$$\tilde{N}_{nj} \equiv (N_R^{int})_{nj} \otimes \mathbb{I}_L^{int} \otimes \mathbb{I}_R^{ext} \otimes \mathbb{I}_L^{ext}, \tag{73}$$

where $\mathbb{I}_L^{int}, \mathbb{I}_R^{ext}, \mathbb{I}_L^{ext}$ are the identity operators in the corresponding Fock spaces. Then, any state in the $\mathscr{F}^{out}$ basis (cf. equation (47)) is now an eigenstate of the collapse operators $\tilde{N}_{nj}$.

We consider the formation of a black hole by the gravitational collapse of an initial matter distribution characterized by a pure quantum state $|\Psi_i\rangle$ describing a localized excitation of the field $\hat{f}$. We assume that there is a compact boundary ∂S_{QG} around the black hole singularity, where a full quantum gravity theory will be needed in order to have a description of the spacetime. Furthermore, we assume that quantum gravity will remove the general relativity singularities without leading to dramatic violations of conservation laws (e.g. energy or momentum), and that the spacetime region emerging at the other side of the singularity is a simple vacuum that can be taken to correspond to a flat Minkowski region. The initial state defined at $\mathscr{I}^-$ corresponding to the vacuum for the right moving modes and the left moving pulse forming the black hole, i.e. $|\Psi_{in}\rangle = |0\rangle_R^{in} \otimes |Pulse\rangle_L$ can be written as

$$|\Psi_i\rangle = N \sum_F e^{\frac{-\pi}{\Lambda}E_F} |F\rangle^{ext} \otimes |F\rangle^{int} \otimes |Pulse\rangle_L \, , \tag{74}$$

where we have used equation (51).

We can assume that the state $|\Psi_i\rangle$ remains almost unchanged as it evolves outside the horizon, since λ is very small until it reaches some hypersurface Σ_{τ_0} described by the spacetime foliation. We proceed to derive the final density matrix for the modified CSL evolution of $|\Psi_i\rangle$, from the initial hypersurface Σ_{τ_0} to Σ_{τ_S}. Hence, for the free field evolution, we have

$$\rho(\tau) = \mathscr{T} e^{-\int_{\tau_0}^{t} dt' \frac{\lambda(\tau')}{2} \sum_{nj} [\underrightarrow{\tilde{N}}_{nj} - \underleftarrow{\tilde{N}}_{nj}]^2} \rho(\tau_0), \tag{75}$$

where

$$\rho(\tau_0) = |0\rangle_R^{in} \langle 0|_R^{in} \otimes |Pulse\rangle_L \langle Pulse|_L = \rho_R(\tau_0) \otimes |Pulse\rangle_L \langle Pulse|_L \, . \tag{76}$$

The evolution operator given in equation 75 acts only on $\rho_R(\tau_0)$. Then, the right-moving initial density matrix $\rho_R(\tau_0)$ can be expressed in terms of the *out* quantization as

$$\rho_R(\tau_0) = N^2 \sum_{F,G} e^{-\frac{\pi}{\Lambda}(E_F + E_G)} |F\rangle_R^{int} \otimes |F\rangle_R^{ext} \langle G|_R^{int} \langle G|_R^{ext} \, . \tag{77}$$

We now have that

$$\sum_{nj} [\underrightarrow{\tilde{N}}_{nj} - \underleftarrow{\tilde{N}}_{nj}]^2 |F\rangle_R^{int} \otimes |F\rangle_R^{ext} \langle G|_R^{int} \otimes \langle G|_R^{ext} = \sum_{nj} (F_{nj} - G_{nj})^2 |F\rangle_R^{int} \otimes |F\rangle_R^{ext} \langle G|_R^{int} \otimes |G\rangle_R^{ext} \, . \tag{78}$$

Since $\tilde{N}_{nj}$ and their eigenvalues do not depend on τ, then for any τ we have

$$\rho_R(\tau) = N^2 \sum_{F,G} e^{-\frac{\pi}{\Lambda}(E_F + E_G)} e^{-\sum_{nj}(F_{nj} - G_{nj})^2 \int_{\tau_0}^{\tau} d\tau' \frac{\lambda(\tau')}{2}} |F\rangle_R^{int} \otimes |F\rangle_R^{ext} \langle G|_R^{int} \otimes \langle G|_R^{ext} \, , \tag{79}$$

which in general is not a thermal state. However, as τ approaches the singularity, we have

$$\int_{\tau_0}^{\tau} d\tau' \lambda(\tau') = \lambda_0 \left(\frac{4\sqrt{M\Lambda} \tanh^{-1}\left(\frac{\Lambda^{3/2}}{\sqrt{M}}\tau\right)}{\mu} + \tau \right)_{\tau_0}^{\tau_S = \frac{\sqrt{M}}{\Lambda^{3/2}}} , \tag{80}$$

which is divergent, since $\lambda(\tau)$ increases with curvature. Thus, as $\tau \to \tau_S$, the non-diagonal elements of $\rho(\tau)$ vanish (i.e. the quantum system loses coherence), and in this limit we have

$$\lim_{\tau \to \tau_S} \rho_R(\tau) = N^2 \sum_F e^{-\frac{2\pi}{\mu} E_F} |F\rangle_R^{int} \otimes |F\rangle_R^{ext} \langle F|_R^{int} \otimes \langle F|_R^{ext} . \tag{81}$$

Thus, as $\tau \to \tau_S$, the density matrix representing the state evolution of equation 74 is given by

$$\lim_{\tau \to \tau_S} \rho_(\tau) = N^2 \sum_F e^{-\frac{2\pi}{\mu} E_F} |F\rangle_R^{int} \otimes |F\rangle_R^{ext} \langle F|_R^{int} \otimes \langle F|_R^{ext} \otimes |Pulse\rangle_L \langle Pulse|_L . \tag{82}$$

Equation (82) represents the ensemble when the evolution almost reaches the singularity (at the hypersurface $\Sigma_{\tau \to \tau_S}$), and E_F is the energy of the state $|F\rangle_R^{ext}$ as measured by late-time observers.

Now if quantum gravity turns the internal state post singularity into a straightforward low energy state, e.g. the vacuum

$$|\Psi_{\tau \to \tau_S}\rangle = |F\rangle_R^{ext} \otimes |F\rangle_R^{int} \otimes Pulse_L \to |F\rangle_R^{ext} \otimes |0\rangle^{post-sing} , \tag{83}$$

then the final state characterizing the ensemble of systems on Σ_f will be

$$\begin{aligned} \rho_{final} &= N^2 \sum_F e^{-\frac{2\pi}{\Lambda} E_F} |F\rangle_R^{ext} \otimes |0^{post-sing}\rangle \langle F|_R^{ext} \otimes \langle 0^{post-sing}| \\ &= |0^{post-sing}\rangle \langle 0^{post-sing}| \otimes \rho_{thermal}^{ext}, \end{aligned} \tag{84}$$

therefore the system has evolved from an initially pure state to a state representing the proper thermal state of radiation.

3 Simplified Model of the Hawking Process

The vacuum of a free quantum field in flat space has Fourier modes of all wavelengths that go down to zero. When gravity is taken into account, the vacuum description is also relative to the observer. Our present discussion is based on the assumption that quantum gravity effects are negligible. For the effects of quantum gravity to become small, we assume that under a certain set of conditions (i.e. the semiclassical physics domain), we can specify the quantum state on an initial spacelike slice, and the state on later slices is given by a Hamiltonian evolution. Furthermore, we assume that the influence of the state in one region on the evolution in another region goes to zero as the distance between the regions goes to infinity, i.e. we assume locality. Hawking's theorem then shows that requiring locality together with these conditions leads to an unacceptable physical evolution.

Specifically, if we require

$$R_s, K, R \ll \frac{1}{l_p^2}, \tag{85}$$

$$U, P \ll l_p^{-4}, \tag{86}$$

$$\frac{dN^i}{ds}, \frac{dN}{ds} \ll \frac{1}{l_p}. \tag{87}$$

where R_s is the intrinsic curvature of a slice, K is the extrinsic curvature of a slice, R is the curvature of the full spacetime in the neighborhood of the slice, U, P are the energy and momentum density respectively, N^i, N are the lapse and shift vectors specifying the evolution and l_p is the Planck length, then we are in a domain of semiclassical physics.

Starting with the vacuum state on the lower slice of figure 3(a), the state on the upper slice is distorted by the black hole geometry such that particle pairs are created where the geometry is being deformed (figure 3(b)). This is due to the natural vacuum state on one slice being different from the one on a later slice. For simplicity, we assume that the geometry in the deformation region is characterized by a scale $L \approx 3$ kM, i.e. the curvature length scale at the horizon of a solar mass black hole. There is also some matter $|\Psi\rangle_M$ on the spacelike slice, very far away from the place of pair creation, which is only weakly correlated with the state of the pair - we consider it is at a distance $L' \ll L$ and take $L' \approx 10^{77}$ lyr, the typical Hawking evaporation time for a solar mass black hole. Note that all these slices satisfy the conditions (85)-(87).

The state of the created particle pair (b, c) is an entangled state of the form given in Giddings & Nelson (1992), which we discussed in section 2.2; here we will consider a simplified form that retains the essence of the entanglement we want to study, i.e.

$$|\Psi_{\text{pair}}\rangle = \frac{1}{\sqrt{2}} |0\rangle_c |0\rangle_b + \frac{1}{\sqrt{2}} |1\rangle_c |1\rangle_b . \tag{88}$$

There is some matter shell collapsed into a black hole $|\Psi\rangle_M$ on the spacelike slice, far away from the place of particle creation; assuming locality, the complete state on a slice after pair

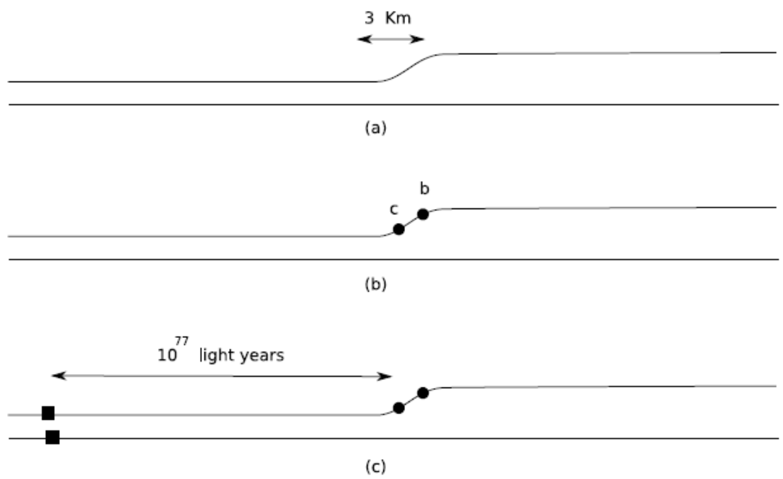

Figure 3: Spacelike Slices in an Evolution - taken from Mathur (2009).

creation has taken place on a slice is

$$|\Psi\rangle \approx |\Psi\rangle_M \otimes \left(\frac{1}{\sqrt{2}}|0\rangle_c|0\rangle_b + \frac{1}{\sqrt{2}}|1\rangle_c|1\rangle_b\right). \tag{89}$$

This means there is always some effect of $|\Psi\rangle_M$ on the state of the created pair that allows only small fluctuations around that state. It is important for Hawking's argument that we make this statement precise. Let $|\Psi\rangle_M = \left(\frac{1}{\sqrt{2}}|\uparrow\rangle_M + \frac{1}{\sqrt{2}}|\downarrow\rangle_M\right)$ consisting of a spin up or down. If there was no effect of $|\Psi\rangle_M$ on the state of the created pairs, then the state on a slice would be

$$|\Psi\rangle \approx \left(\frac{1}{\sqrt{2}}|\uparrow\rangle_M + \frac{1}{\sqrt{2}}|\downarrow\rangle_M\right) \otimes \left(\frac{1}{\sqrt{2}}|0\rangle_c|0\rangle_b + \frac{1}{\sqrt{2}}|1\rangle_c|1\rangle_b\right). \tag{90}$$

Locality allows small departure from this state, e.g.

$$|\Psi\rangle = \left(\frac{1}{\sqrt{2}}|\uparrow\rangle_M + \frac{1}{\sqrt{2}}|\downarrow\rangle_M\right) \otimes \left[\left(\frac{1}{\sqrt{2}} + \epsilon\right)|0\rangle_c|0\rangle_b + \left(\frac{1}{\sqrt{2}} + \epsilon\right)|1\rangle_c|1\rangle_b\right]. \tag{91}$$

Writing the density matrix (improper mixture) describing the quantum b, while tracing over the unobserved degrees of freedom in M and c, we find the entanglement entropy of equation (90) to be

$$S_{\text{ent}} = -\text{tr}[\rho \ln \rho] = \ln 2, \tag{92}$$

and for equation (91)

$$S_{\text{ent}} = -\text{tr}[\rho \ln \rho] = \ln^2 - \epsilon^2(6 - 2\ln 2) \approx \ln 2. \tag{93}$$

In the semiclassical limit, therefore, locality yields

$$\frac{S_{\text{ent}}}{\ln 2} - 1 \ll 1. \tag{94}$$

We now apply the discussion above to a Schwarzschild black hole with the time-independent metric

$$ds^2 = -\left(1 - \frac{2M}{r}\right)dt^2 + \left(1 - \frac{2M}{r}\right)^{-1} dr^2 + r^2(d\theta^2 + \sin^2 d\phi^2). \tag{95}$$

Note that we ignore the backreaction effects and consider that the black hole is described by this metric, except for when it becomes Planck sized. The curvature R in the vicinity of the horizon is $R \sim 1/M^2$. We consider that the horizon is 'information free'. Specifically, a point on the horizon is information free if around this point we can find a neighborhood which is the 'vacuum', in the sense that the evolution of field modes with wavelengths $l_p \ll \lambda \lesssim M$ is QFT-CS semiclassical up to terms that vanish as $m_p/M \to 0$. (There is no unique definition of particles in any curved spacetime, however if the curvature radius is R, then for wavemodes with wavelength $\lambda \lesssim R$, we can define particles such that 'empty' space can be interpreted. Thus, 'empty' space within this definition means two different particle descriptions will only vary by ~ 1 quanta with $\lambda \sim R$.

We define now the slicing of the black hole geometry in a simplified, but analogous manner with section 2.5. For $r > 4M$, we let the slice be $t = t_1$ constant. Inside the black hole, the spacelike slices are $r =$ constant instead, so for $r = r_1$, we let $M/2 < r_1 < 3M/2$, such that this part of the slice is not near the horizon or the singularity. These two parts are then joined by a smooth connector segment $\mathscr{C}$ that satisfies conditions (85)-(87). In the case of a shell of mass M collapsing towards the origin $r = 0$ as defined in section 2.1, we can follow the $r = r_1$ part to early times before the formation of the black hole and extend it to $r = 0$ (no singularity here yet).

The evolution to a later slice S_2 is made by taking $t = t_1 + \Delta$ for $r > 4M$ and $r = r_1 + \delta$, with $\delta \ll M$ for the $r =$ constant part. These two parts are again joined by a smooth connector $\mathscr{C}$ that is the same for all slices in the limit $\delta \to 0$. Note that the $r =$ constant part of the later slice S_2 has to be longer than the $r =$ constant part of the initial slice S_1, as seen from figure 5. This extra part of the slice is needed, since the connector joins the $r =$ constant and $t =$ constant parts, and the $t =$ constant has been evolved forwards on the later slice. At early times, the $r =$ constant part is extended smoothly to $r = 0$, where there is no singularity yet.

The evolution between S_1 and S_2 is easily described in terms of the lapse and shift vectors on the spacetime: we take the slice S_1 and pick a point $x^i \in S_1$, move along the timelike normal until we reach a point on S_2, and let the point on S_2 have the same spatial coordinates x^i. Thus, the shift vector is set to be $N^i = 0$. With this choice, there is no change in intrinsic geometry in the $t =$ constant part and this part of the slice advances forward with a lapse function $N = (1 - 2M/r)^{1/2}$. In the limit $\delta \to 0$, the $r =$ constant part of S_1 moves over to S_2 with no change in intrinsic geometry. The early time part extending to $r = 0$ also remains unchanged. The connector segment will 'stretch' during the evolution, since S_2 has

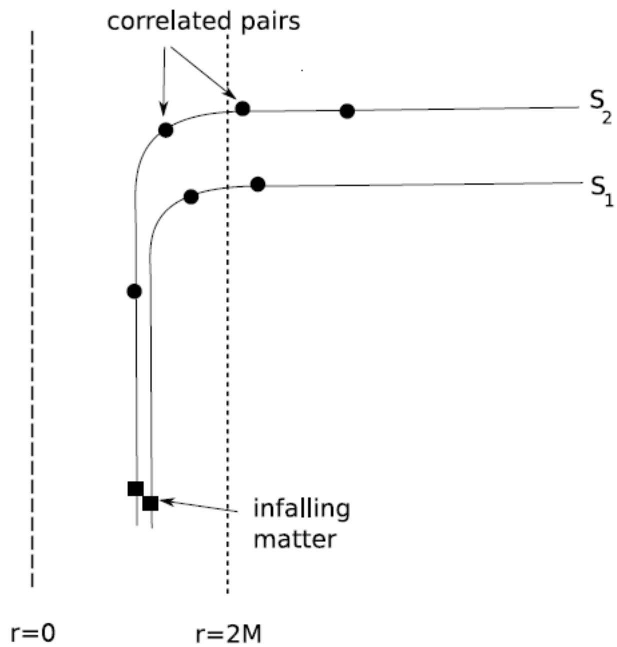

Figure 4: Coordinate Evolutions for Spacetime Slices - taken from Mathur (2009).

to account for an extra $r =$ constant part. This stretching happens only in the neighborhood of the connector, taken in this example to be $\sim 3\,\mathrm{kM}$ for a solar mass black hole.

A succession of such slices S_n of this type can be considered, with the evolution from S_n to S_{n+1} defined in analogous way as above; all these slices satisfy the conditions (85)-(87). The evolution of successive slices leads to creation of particle pairs which is entangled in a specific way which we show below. The pair members that float out to infinity are called Hawking radiation. This is to be contrasted with normal hot body radiation, where the photons are emitted from the hot body itself. In the black hole case, the particle pairs are the result of Fourier modes stretching to larger wavelengths, thus forcing a particle pair to be 'pulled out of the vacuum'. This is not the case in Minkowski space, where the evolved slices will not be spacelike everywhere. Because the space and time directions interchange inside the black hole horizon, particles will keep being produced in a Schwinger-type process (which moves $|\Psi\rangle_{\mathrm{M}}$ further away from the place of pair creation and also moves the earlier created quanta away from the place of pair creation) until the hole becomes very small.

After N steps analogous to equation (90), we will have that the stretching of the connector segment creates new correlated pairs (b_i, c_i), while the earlier created pairs move away from

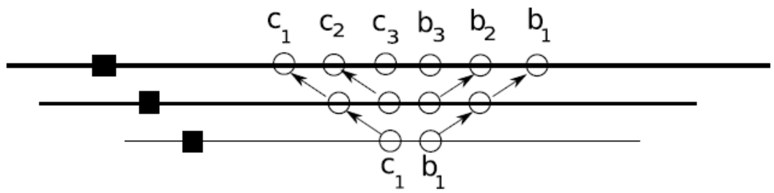

Figure 5: The Creation of Hawking Pairs - taken from Mathur (2009).

each other and from the region of stretching, so the complete state on a slice is

$$|\Psi\rangle \approx |\Psi\rangle_M \otimes \left(\frac{1}{\sqrt{2}}|0\rangle_{c_1}|0\rangle_{b_1} + \frac{1}{\sqrt{2}}|1\rangle_{c_1}|1\rangle_{b_1}\right) \otimes \left(\frac{1}{\sqrt{2}}|0\rangle_{c_2}|0\rangle_{b_2} + \frac{1}{\sqrt{2}}|1\rangle_{c_2}|1\rangle_{b_2}\right)\cdots$$
$$\cdots \otimes \left(\frac{1}{\sqrt{2}}|0\rangle_{c_n}|0\rangle_{b_n} + \frac{1}{\sqrt{2}}|1\rangle_{c_n}|1\rangle_{b_n}\right). \tag{96}$$

The space b_i is entangled with M, c_i with

$$S_{\text{entanglement}} = n \ln 2. \tag{97}$$

As the quanta b_i collect at infinity, the mass of the black hole decreases. We stop evolving the spacelike slices when $M_{\text{BH}} \sim m_{\text{Planck}}$. Slicing the black hole geometry forces us into either:

- Mixed states: The black hole evaporates completely and the quanta b_i have a non-zero entanglement entropy. But since there is nothing left that they are entangled with, the final state is not described by any quantum wavefunction. The final state can only be described by a density matrix.

- Remnants: The evolution stops when $M_{\text{BH}} \sim m_{\text{remnant}}$. Thus, given the entanglement calculated above, we find that the theory contains remnants, if we allow for an arbitrarily high entanglement with systems far away from the remnant. This, however, is not the expected behaviour of usual quantum systems, because the remnants have unbounded degeneracy, while having energy and size within bounds.

We now comment on the problem of small corrections to the leading order state that come from small interactions between the earlier created pairs and the newly created pair. The matter shell $|\Psi\rangle_M$ is very far away on the spacelike slice, but it could have small effects on the pair being created, thus removing the entanglement between the quanta b_i and the (M, c_i) inside the black hole. If this happens, there is no paradox, since the black hole containing M, c_i can vanish, and we are left with pure quanta b_i carrying all the information about the initial state of $|\Psi\rangle_M$. It can be shown via entropy subadditivity (see Mathur 2009) that the small corrections to the leading order state cannot remove this problem, and the entanglement keeps growing - analogously, in section 2, it is argued by Giddings & Nelson (1992) that to leading order in perturbation theory the effect of the backreaction is to modify the Bogolyubov transformation, but not in a way that restores information lost to the black hole. The same result is obtained by Fabbri & Navarro-Salas (2005); by a careful accounting of the ingoing and outgoing modes, they also obtain an independent emission in frequencies of entangled quantum states representing outgoing and incoming radiation and no correlations between particles emitted in different modes. The correlations needed to ensure the purity if the *in* vacuum are in agreement with the thermal emission results. The first possibility then leads to a loss of QM unitarity, since a pure initial state evolves to a mixed final state. Possibility 2 differs from expected physics. The Hawking argument cannot say which of these possibilities will occur, since the semiclassical treatment breaks down at the endpoint of evolution.

Working in the CSL dynamics framework described in section 2.5 we have that for n pairs of entangled particles,

$$\rho = |\Psi\rangle \langle\Psi| = |\Psi\rangle_M \langle\Psi|_M \otimes \bigotimes_{i=1}^{n} \left[\left(a^2 |0\rangle_{\text{out}} |0\rangle_{in} + b^2 |1\rangle_{out} |1\rangle_{in} \right) \left(a^2 \langle 0|_{out} \langle 0|_{\text{in}} + b^2 \langle 1|_{out} \langle 1|_{in} \right) \right]_i , \tag{98}$$

where a and b are standard quantum mechanical amplitudes. As a result of the system being in contact with the black hole and losing coherence, the cross terms resulting from multiplying the brackets vanish, and we are left with

$$\rho = |\Psi\rangle \langle\Psi| = |\Psi\rangle_M \langle\Psi|_M \otimes \left[\bigotimes_{i=1}^{n} a^{2n} \left(|0\rangle_{out} |0\rangle_{in} \langle 0|_{out} \langle 0|_{in} \right)_i + b^{2n} \bigotimes_{i=1}^{n} \left(|1\rangle_{out} |1\rangle_{in} \langle 1|_{out} \langle 1|_{in} \right)_i \right]. \tag{99}$$

Hence, the density matrix describing the particle pairs represents an improper statistical mixture (the subsystem of a larger system that is in a pure state) obtained by tracing out the unobserved matter degrees of freedom $|\Psi\rangle_M \langle\Psi|_M$. Resolving the paradox, then, requires one to explain how a pure state becomes a proper thermal state, rather than an improper one, simply because the region corresponding to the black hole interior will eventually disappear. Decoherence destroys the ability of a state to make interference patterns with itself and thus converts quantum probabilities into classical probabilities; there is no wavefunction that can yield such a density matrix. The particles' density matrix describes the classical probabilities a^{2n} for having a $|0\rangle_{out} |0\rangle_{in}$ state and b^{2n} for having a $|1\rangle_{out} |1\rangle_{in}$ state. So far, we have obtained an improper statistical mixture by tracing out the environment. Decoherence gives the right classical probabilities, but does not tell what happens to the system itself upon measurement - this is the key conundrum of the quantum measurement problem. In this context, the wavefunction collapse model we have considered in this paper has been specifically designed to collapse the state of the system onto a definite outcome, by implementing stochastic modifications to the evolution equation describing how the state of the particles changes in time. As a result of the CSL evolution, when the black hole evaporates, assuming that the singularity is replaced by a straightforward low-energy state, we will obtain a proper statistical mixture representing thermal emission of particles of the form

$$\rho = |\Psi_{\text{post-sing}}\rangle \langle\Psi_{\text{post-sing}}| \otimes e^{E/kT} \bigotimes_{i=1}^{n} \left[a^2 \, |0\rangle_{\text{out}} \, \langle 0|_{\text{out}} + b^2 \, |1\rangle_{\text{out}} \, \langle 1|_{\text{out}} \right]_i , \tag{100}$$

where all the ingoing particle states have been collapsed by the CSL operators.

4 Dark Matter Production from Primordial Black Holes

4.1 General Cosmological Setting

The standard ΛCDM model assumes that the different fluids in the Universe are matter made of a mixture between dark matter and baryonic matter, radiation composed of relativistic particle species e.g. photons, neutrinos, and dark energy, which is an unidentified negative pressure component currently driving the expansion of the Universe today; at the beginning of the Universe radiation was dominant. In the standard cosmological model, the dark matter (DM) is cold, i.e. with small velocities and the dark energy is considered to be a "cosmological constant" (Λ) with constant density and equation of state $\rho_\Lambda = -P_\Lambda$, forming the CDM paradigm (Pontzen & Peiris 2020).

In the context of particle physics, dark matter can be made of several new particles which are expected to be electrically neutral, uncoloured, weakly-interacting and stable. One of the most important cosmological observables connecting DM, cosmology and particle physics is the cosmological density of dark matter i.e. the relic density. Dark matter particles, originating from the early Universe, have been interacting with the thermal bath before decoupling from it, they may have decayed/annihilated and we observe the particles which have survived until now - the relics. There exist several models that connect the relic dark matter density to the primordial Universe. Since dark matter density has been precisely measured by cosmological observations, we can use it to set constraints on particle physics models, but also on early Universe scenarios (Arbey & Mahmoudi 2021).

Dark matter is massive, stable over billions of years, very likely collisionless, interacting mostly gravitationally and separate from baryonic matter. The terms "cold" and "hot" are used to characterize nonrelativistic and relativistic species, respectively. Beside baryons, the only electromagnetically (EM) neutral, stable massive particles that exist in the SM are neutrinos, which are a good example of hot DM. Since hot DM is composed of massive and high velocity components, it tends to spread structures such as galaxies, therefore if all dark matter was hot, structures would be shaped differently from what we observe and the Cosmic Microwave Background (CMB) anisotropies would have larger sizes. Hence, hot dark matter can only account for a small part of the total dark matter; under the CDM assumption, it is considered that the whole dark matter content is cold. Even cold dark matter is a broad term which can include from weakly-interacting massive particles (WIMPs) of new physics models to primordial black holes. The masses of dark matter candidates span the range given in the figure 6 below.

We now define some important cosmological quantities for the present discussion: the Hubble parameter is a measure of the temporal (extrinsic) curvature of the FRW geometry, and it is defined through the first Friedmann equation as

$$\frac{\dot{a}}{a} \equiv H^2 = \frac{8\pi G}{3}\rho - \frac{K}{a^2} + \frac{\Lambda}{3}, \tag{101}$$

where H is the Hubble parameter, a is the cosmological scale factor, K is the curvature, ρ is the energy density and Λ is the cosmological constant as it appears in Einstein's equations.

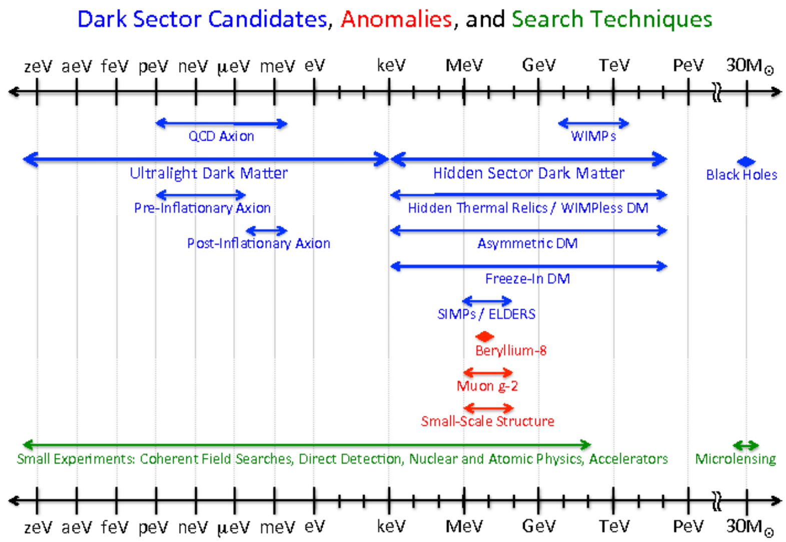

Figure 6: Dark Matter Mass Ranges - taken from Battaglieri et al. (2017).

The second Friedmann equation relates the Universe's expansion to pressure, density and the cosmological constant as

$$\frac{\ddot{a}}{a} = \dot{H} + H^2 = -\frac{4\pi G}{3}(\rho + 3p) + \frac{\Lambda}{3}. \tag{102}$$

As a consequence of the conservation of energy-momentum tensor, we get a third independent equation describing the dynamics, called the continuity equation,

$$\dot{\rho} + 3H(\rho + p) = 0. \tag{103}$$

From the first Friedman equation we have for $\Lambda = 0$ a critical density $\rho_c(t) = 3H^2(t)/8\pi G$ for which the Universe appears flat. We also have that for different cosmological fluids, the equation of state is

$$p = w\rho, \tag{104}$$

where w is called the adiabatic index. From the equation of state and the continuity equation, we derive

$$\rho(t) \propto a(t)^{-3(w+1)}, \tag{105}$$

which holds for any fluid, irrespective of the geometry of spacetime. This allows us to describe the behaviour of the density as a function of the scale factor and distinguish between radiation, matter and vacuum/dark energy dominated eras, assuming that $a(t = 0) = a_0 = 1$ today. This indicates the existence of a singularity in the finite past - the Big Bang. This conclusion relies on the assumption that GR (and consequently the Friedmann equations)

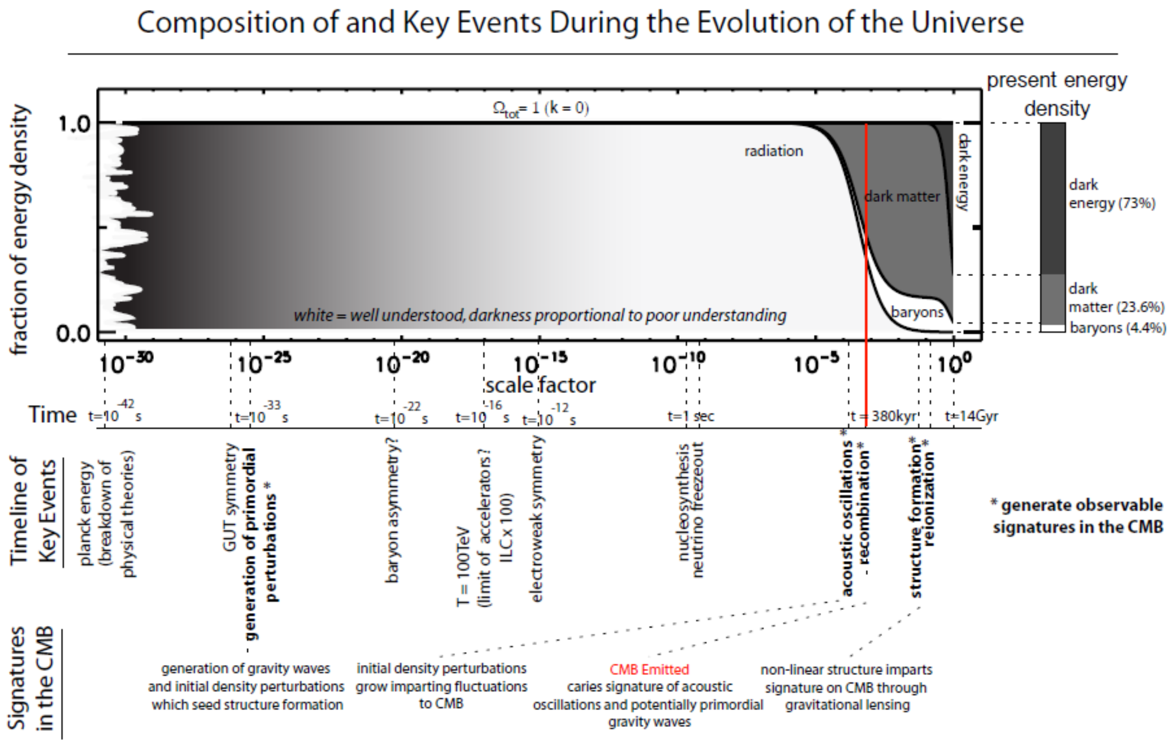

(a)

Figure 7: Important Timesteps in the Cosmological Evolution - taken from Pontzen & Peiris (2020).

are applicable up to high energies - it is expected that a quantum theory of gravity will remove the initial Big Bang singularity. Even today, theories like inflation discussed below dramatically alter the classical Big Bang picture, by violating the strong energy condition.

Originally, the idea of inflation was introduced to solve three problems of the Big Bang theory: the first is the apparent flatness of the Universe. We observe that the curvature $K \approx 0$, but its exact value is unknown. The curvature density may represent a small fraction of the critical density and we know that it evolves as $\rho \propto a^{-2}$, whereas the matter and radiation densities evolve as $\rho \propto a^{-3}$ and $\rho \propto a^{-4}$, respectively. Therefore, curvature always had a negligible effect in comparison to matter and radiation. Yet curvature is related to gravity, thus one can suppose that there existed a small non-negligible curvature at the beginning of the Universe. In such a case, because of the evolution of the curvature density, curvature would dominate the expansion today, contrary to the observations. The second problem is about the isotropy of the CMB. The expansion of the Universe is a global dilatation, so the apparent velocity of a fixed object at a distance r from us is given by $v = Hr$. If this velocity becomes larger than the speed of light, a horizon forms, delimiting causally disconnected regions. The corresponding radius $rH = c/H$ is called the Hubble radius. Integrating from the beginning of the Universe until recombination, it is possible to show that the Hubble radius at the beginning of the Universe corresponds to regions of about 2° in the CMB sky. Therefore, we should observe CMB anisotropies of angular sizes close to this value. This is in contradiction with the measured isotropy of the CMB which is of the order 10^{-5}. The third problem is related to the CMB anisotropies themselves. Starting from a purely homogeneous and isotropic Universe, it is not possible to generate inhomogeneities. It has been shown that quantum fluctuations cannot account for the size of the inhomogeneities which seeded large scale structures and imprinted the CMB - one of the most important cosmological constraints obtained from CMB measurements is on the power spectrum corresponding to the mass density contrast as a function of scale (which is a Fourier transform of the matter correlation function). Hence, the temperature fluctuations in the CMB can be seen as markers of small-size matter density contrast and CMB data can also be used to extend the power spectrum to lower scales. The Planck combined results are consistent with LSS data and show that the ratio of baryonic mass over total matter mass is ≈ 15, in agreement with the results at galaxy and galaxy cluster scales.

The three problems mentioned above are theoretically resolved by the scenario of inflation, which occurred $\approx 10^{36}$ seconds after the beginning of the Universe; here the Universe underwent an exponential expansion called inflation. Inflation could be driven by the presence of a scalar field, the inflaton, which decayed into standard particles at the end, during the so-called reheating period. Because of this exponential expansion, regions originally causally connected before inflation have been causally disconnected, thus the apparent isotropy of the CMB results from the causal connection between the different regions of the sky in the pre-inflation period. Also to generate an exponential expansion, the inflaton had to be dominant with a nearly constant density, so that any curvature existing in the early Universe would be flattened by the expansion and the effective curvature density has rapidly become negligible. Finally, during reheating, quantum fluctuations have also been enlarged by the rapid expansion resulting in large enough inhomogeneities to seed the formation of large scale structures. The inflation mechanism is described by a scalar field Lagrangian

$$\mathcal{L}_\phi = g^{\mu\nu}\partial_\mu\partial_\nu\phi - V(\phi), \tag{106}$$

which gives in terms of density and pressure in the Friedmann-Lemaître Universe

$$\begin{aligned} \rho_\phi &= \frac{1}{2}\cdot\phi^2 + V(\phi), \\ P_\phi &= \frac{1}{2}\cdot\phi^2 - V(\phi). \end{aligned} \tag{107}$$

In order to reach an exponential expansion, the field needs to have a slowly-varying density resulting in a negative pressure, an equation of state $w \approx -1$, a negligible kinetic term and a dominating potential. Then, the scalar field is slowly rolling down the potential (such a model is called slow-roll inflation) and requires the slow-roll parameters to satisfy $\epsilon, |\eta| << 1$, where

$$\epsilon = \frac{M_P^2}{16\pi}\left(\frac{V'}{V}\right)^2, \quad \eta = \frac{M_P^2}{8\pi}\left(\frac{V''}{V}\right). \tag{108}$$

At the end of inflation, the field reaches the minimum of the potential and starts oscillating around the minimum. If coupled to the Standard Model, the field decays into SM particles, following the modified Klein-Gordon equation,

$$\ddot{\phi} + 3H\dot{\phi} + \frac{dV}{d\phi} = \xi_\phi \rho_\phi, \tag{109}$$

where ξ is the decay width of the scalar field. If the field decays into radiation, then the radiation receives an entropy injection,

$$\frac{ds_{\mathrm{rad}}}{dt} = -3Hs_{\mathrm{rad}} + \frac{\xi_\phi \rho_\phi}{T}, \tag{110}$$

resulting in reheating of the primordial plasma. The reheating temperature T_{RH} of the scalar fields reads

$$\xi_\phi = \sqrt{\frac{4\pi^3 g_{\mathrm{eff}}(T_{\mathrm{RH}})}{45}} \frac{T_{\mathrm{RH}}^2}{M_P}, \tag{111}$$

where g_{eff} is the effective number of degrees of freedom of radiation.

In considering a new physics scenario, we assume that the dark matter is made of one single type of particles, and the new physics particles are protected by a discrete symmetry, so that new particles are produced in pair. The particles also follow a Maxwell-Boltzmann distribution. From the Friedmann equation (101), we have that

$$\rho_{\mathrm{rad}}(T) = g_{\mathrm{eff}}(T) \frac{\pi^2}{30} T^4. \tag{112}$$

The factor $g_{\mathrm{eff}}(T)$ for all relativistic species can be calculated as the sum

$$g_{\mathrm{eff}}(T) = \sum_{i=b} g_i \left(\frac{T_i}{T}\right)^4 + \frac{7}{8} \sum_{i=f} g_i \left(\frac{T_i}{T}\right)^4, \tag{113}$$

where the first term is a sum over all bosons and the second a sum over all fermions (the relative factor 7/8 accounts for the difference in Fermi and Bose statistics) (Kolb & Turner 1990). Below the electron mass, only the photon ($g_\gamma = 2$) and three left-handed neutrinos contribute, so that $g_{\mathrm{eff}} = 7.25$.Below the muon mass, the electron and also the positron have to be included, so that $g_{\mathrm{eff}} = 10.75$. For the full SM, here defined to include three light left-handed neutrinos, $g_{\mathrm{eff}} = 106.75$. At higher temperatures, g_{eff} will be model-dependent. If we include the (massless) graviton, this has the effect of adding 2 units to the previous values of g_{eff} (Masina 2021). In an expanding Universe, the entropy density can be written as

$$s = \frac{\rho + p}{T}, \tag{114}$$

so the entropy density is dominated by the contribution of relativistic particles and can be approximated to (Kolb & Turner 1990)

$$s(T) = h_{\mathrm{eff}}(T) \frac{2\pi^2}{45} T^3, \tag{115}$$

where h_{eff} is the effective number of entropic degrees of freedom of radiation. Therefore, we have

$$g_{\text{eff,s}} = \sum_{i=b} g_i \left(\frac{T_i}{T}\right)^3 + \frac{7}{8} \sum_{i=f} g_i \left(\frac{T_i}{T}\right)^3. \tag{116}$$

Conservation of entropy implies $S \propto R^{-3}$, for radius R, therefore $g_{\text{eff,s}} T^3 R^3$ remains constant as the Universe expands and the physical size of a comoving volume element is $\propto R^3 \propto s^{-1}$. Thus, the yield of a particle species in terms of the ratio of the number density to the radiation entropy density is

$$Y(T) = \frac{n(T)}{s(T)}. \tag{117}$$

The evolution of the entropy density is then specified by

$$s(a) = \frac{2\pi^2}{45} g_{\text{eff,s}} T(t_{RH})^3 \cdot \left(\frac{a_{RH}}{a}\right)^3, \tag{118}$$

where a_{RH} is the scale factor at the time of reheating, t_{RH}. If the number of a given species in a comoving volume is not changing, i.e. particles of that species are not being created or destroyed, then $Y(T)$ remains constant. The relic density of dark matter is then

$$\Omega_{DM} h^2 = \frac{m_{DM} s(T_0) Y(T_0) h^2}{\rho_c^0}, \tag{119}$$

where ρ_c^0 is the critical density of the Universe and $h = 0.6774$ is the reduced Hubble parameter. From current observations, $\Omega_{DM} h^2 = 0.11933 \pm 0.00091$.

4.2 Primordial Black Hole Formation

Primordial black holes (pBHs) may have formed in the early Universe from quantum fluctuations that reenter the horizon and collapse. If so, they can have observational consequences at the present epoch, either from Hawking evaporation effects or from a contribution to the present dark matter density (Hawking 1971).

Two ways of calculating the abundance of pBHs formed from a given initial power spectrum is the Press-Schechter formalism, used in large-scale structure studies, where the density field is smoothed on a mass scale M (taken to be at horizon crossing), and the regions where the density contrast exceeds a threshold value Δ_{th} are assumed to form pBHs of mass M. However, the correct value of the threshold is uncertain.

A new approach to the formation of individual primordial black holes based on metric perturbation criteria (instead of density field) and in a form which can be applied to superhorizon initial perturbations is Peak Theory, used in the present paper. This is a criterion formulated by Shibata & Sasaki (1999) in terms of whether the initial central value of a particular metric perturbation variable ψ exceeds a threshold value. Following Green et al. (2004), we consider the metric variable ψ from the spatial part of the metric on uniform-expansion hypersurfaces as

$$g_{ij} = a^2\psi^4\zeta_{ij}, \tag{120}$$

where γ_{ij} is the metric on spatial 3-sections. In the following we assume a flat background and consider only scalar perturbations. Therefore, it can be shown numerically (for further details see Shibata & Sasaki, 1999) that pBH formation takes place if the central value of ψ, denoted ψ_0 exceeds a threshold value $\psi_{0,th}$. We relate the threshold criterion to standard linear perturbation theory quantities, where the spatial part of the metric is given by

$$g_{ij} = a^2[(1+2\mathcal{R})\delta_{ij} + 2\partial_i\partial_j H_T], \tag{121}$$

where $\mathcal{R}$ is the curvature perturbation and H_T is the anisotropic part. Then, the gauge-invariant curvature perturbation on uniform-density hypersurfaces γ is defined as

$$\zeta = \mathcal{R} - H\frac{\delta\rho}{\dot{\rho}}, \tag{122}$$

where H is the Hubble parameter given in equation (101), ρ and $\delta\rho$ are the background density and perturbed density, respectively. We therefore have

$$g_{ij} = a^2(1+2\zeta)\delta_{ij}, \tag{123}$$

on superhorizon scales, where the anisotropic part H_T is negligible (on large scales uniform density hypersurfaces coincide with uniform expansion hypersurfaces). By definition, $\psi^4 = e^{2\Delta N}$, where N is the difference in e-foldings between uniform expansion hypersurfaces, therefore in the quasi-linear regime we have that $e^{2\zeta} = \psi^4$. Arguably, uniform expansion and uniform density slices are almost equivalent even in non-linear regimes, such that $\zeta = \Delta N$. From this, we find that the threshold values of $\psi_{0,th}$ of 1.4 and 1.8 correspond to thresholds on ζ of 0.7 and 1.2, respectively.

4.2.1 Standard Calculation - Press-Schechter

The standard pBH abundance calculation refers to the density contrast on the comoving slicing denoted by Δ, smoothed on a scale R. Integrating the probability distribution $P(\Delta(R))$ over the range of perturbation sizes that form pBHs $\Delta_{th} < \Delta(R) < \Delta_{cut}$, where the upper limit arises from the fact that very large perturbations would correspond to a separate closed universe in the initial conditions (however this cut-off is not significant due to the rapid decrease of $P(\Delta(R))$ as a function of $\Delta(R)$. Using the equation of state (104), we take the threshold density as $\Delta_{th} > w$ (cannot be valid in the limit $w \to 0$, but it is acceptable for e.g. radiation domination where $w = 1/3$).

The smoothed density contrast $\Delta(R, \mathbf{x})$ is found by convolving the density contrast $\Delta(\mathbf{x})$ according to

$$\Delta(R, \mathbf{x}) = V^{-1} \int W(|\mathbf{x}' - \mathbf{x}|/R)\Delta(\mathbf{x}')d^3x', \tag{124}$$

where R is the smoothing scale, $W(y)$ is the window function used for the smoothing and V is the volume of the window function. For Gaussian initial perturbations, the smoothed density perturbation will also inherit the same distribution, therefore

$$P(\Delta(R)) = \frac{1}{\sqrt{2\pi}\sigma_\Delta(R)} \exp\left(- \frac{\Delta^2(R)}{2\sigma^2(R)} \right), \tag{125}$$

where $\sigma_\Delta(R)$ is the variance of $\Delta(R, \mathbf{x})$, i.e.

$$\sigma^2_\Delta(R) = \int_0^\infty W^2(kR)\mathcal{P}_\Delta(k)\frac{dk}{k}. \tag{126}$$

The quantity $\mathcal{P}_\Delta(k) \equiv (k^3/2\pi^2)\langle|\Delta_k|^2\rangle$ is the power spectrum of Δ with $W(kR)$ the volume-normalized Fourier transform of the window function used for smoothing Δ. It is convenient to use the window function

$$W(kR) = \exp\left(- \frac{k^2R^2}{2} \right). \tag{127}$$

On comoving hypersurfaces, we have the useful relation between the density perturbation and the curvature perturbation

$$\Delta(t, k) = \frac{2(1+w)}{5+3w}\left(\frac{k}{aH}\right)^2 \mathcal{R}_c(k), \tag{128}$$

where $\mathcal{R}_c$ is the curvature perturbation on comoving hypersurfaces, which is the same as the curvature perturbation on uniform density hypersurfaces on large scales. The power spectra are related by

$$\mathcal{P}_\Delta(k, t) = \frac{4(1+w)^2}{(5+3w)^2}\left(\frac{k}{aH}\right)^4 \mathcal{P}_{\mathcal{R}_c}(k). \tag{129}$$

At horizon crossing, we have

$$\mathcal{P}_\Delta(k) = \frac{4(1+w)^2}{(5+3w)^2}\mathcal{P}_{\mathcal{R}_c}(k). \tag{130}$$

Therefore, the fraction of the Universe that exceeds the pBH formation threshold $\Delta(M) > \Delta_{th}$ when smoothed on a scale M and forms a black hole of mass $> M$ is given in Press-Schechter theory by

$$\Omega_{\text{pBH,PS}}(\Delta_{th} > M) = 2\int_{\Delta_{th}}^{\infty} P(\Delta(M))d\Delta(M) = \text{erfc}\left(\frac{\Delta_{th}}{\sqrt{2}\sigma_{\Delta}(M)}\right), \tag{131}$$

assuming that the pBH mass is equal to the horizon mass M_H corresponding to the smoothing scale. The factor of 2 in the expression above results from allowing for pBH formation in overdense regions with respect to the mean cosmological density. The Press-Schechter approach generally assumes a power-law primordial power spectrum, i.e.

$$\mathcal{P}_{\mathcal{R}_c}(k) = A_{\mathcal{R}_c}(k/k_0)^{n-1}, \tag{132}$$

which implies

$$\sigma_{\Delta}^2(M) = \frac{2(1+w)^2}{(5+3w)^2}\frac{A_{\mathcal{R}_c}\Gamma[(n-1)/2]}{(k_0R)^{n-1}}. \tag{133}$$

4.2.2 Calculation Using Peaks Theory

We assume that the pBHs are produced in a post-inflationary epoch before the BBN. The use of the Press-Schechter formalism considers the average of the density contrast field , and sum its probability for values above the threshold for the formation of the black hole, which was instead defined for the unsmoothed density contrast field. The peaks theory formation criterion is expressed in terms of the peak value of the fluctuation ψ_0 at some early time when the perturbation is on superhorizon scales. In the following, we will apply the peaks theory to the initial value of ζ to calculate the mass function. After smoothing the density field on a scale M, the number density of peaks with height $> \nu = \zeta_{th}/\sigma_{\zeta}(M)$ is, for high peaks, given by

$$n_{\text{peaks}}(\nu, M) = \frac{1}{(2\pi)^2}\left(\frac{\langle k^2\rangle(M)}{3}^{3/2}(\nu^2-1)e^{-\nu^2/2}\right), \tag{134}$$

where $\langle k^2\rangle(M)$ is the second moment with respect to k of the power spectrum

$$\langle k^2\rangle(M) = \frac{1}{\sigma_{\zeta}^2(M)}\int_0^{\infty} k^2W^2(kR)\mathcal{P}_{\gamma}(k)\frac{dk}{k}. \tag{135}$$

For the power-law spectrum (132) with $A_{\mathcal{R}_c} = A_{\zeta}$ (since $\zeta = \mathcal{R}_c$ on superhorizon scales) and a Gaussian window function, we have

$$\langle k^2\rangle(M) = \frac{n-1}{2R^2}. \tag{136}$$

Hence, the number density of peaks with height $> \nu$, when smoothed with a Gaussian filter on a scale M is

$$n_{\text{peaks}}(\nu, M) = \frac{1}{(2\pi)^2}\frac{(n-1)^{3/2}}{6^{3/2}R^3}(\nu^2-1)e^{-\nu^2/2}, \tag{137}$$

where

$$\nu = \left(\frac{2(k_0 R)^{n-1}}{A_\zeta \Gamma[(n-1/2)]} \right)^{1/2} \zeta_{th}. \tag{138}$$

The number density of peaks is related to the fraction of the Universe in peaks above threshold by $\Omega_{pBH,\text{peaks}}(\nu > M) = n_{\text{peaks}}(\nu, M)M/\rho$. Here M is the mass associated with the filter (which for a Gaussian window function is $M = \rho(2\pi)^{3/2}R^3$, so that

$$\Omega_{\text{pBH,peaks}}(\nu > M) = \frac{(n-1)^{3/2}}{(2\pi)^{1/2}6^{3/2}} \left(\frac{\zeta_{th}}{\sigma_\zeta(M)} \right)^2 \exp\left(-\frac{\zeta_{th}^2}{2\sigma_\zeta^2(M)} \right), \tag{139}$$

where

$$\sigma_\zeta(M) = \frac{5+3w}{2(1+w)} \sigma_\Delta(M) = \left(\frac{A_\zeta \Gamma[(n-1)/2]}{2(k_0 R)^{n-1}} \right)^{1/2}. \tag{140}$$

4.3 Dark Matter Genesis via Hawking Decay

4.3.1 Schwarzschild Black Holes

As first shown by Hawking (1971), a spherically symmetric black hole with mass $M \equiv M_{10} \times 10^{10}$g emits thermal radiation with temperature (Arbey et al. 2020)

$$T_{\text{Schw}} = \frac{1}{8\pi GM} \approx 1.06 M_{10}^{-1} \text{ TeV}, \tag{141}$$

assuming that the hole has no charge or angular momentum. In the first part of the paper, we assumed that the field $\hat{f}$ propagates as a pure free field, without feeling the black hole potential $V_l(r)$. By neglecting the potential, one would find that the emitted energy flux (i.e. luminosity $\mathcal{L}$) receives a divergent contribution of angular momenta from the field. The effect of the potential (i.e. the backscattering) is to modify the pure Planckian spectrum by a factor $\Gamma_{\omega l}$, such that the total luminosity is

$$\mathcal{L} = \frac{1}{2\pi} \int_0^\infty d\omega \frac{\hbar\omega}{e^{8\pi M\omega} - 1} \sum_{l=0}^{\infty} (2l+1)\Gamma_{\omega l}, \tag{142}$$

where $\Gamma_{\omega l} = |\mathcal{T}_l(\omega_l)|^2$ represents the greybody factor, defined in terms of the transmission amplitude within a created pair, with one quanta of the pair crossing the horizon just after its formation, while the other quanta reaching $\mathscr{I}^+$, with amplitude $\mathcal{T}_l$ or being scattered back into the horizon with amplitude $\mathcal{R}_l$ (Fabbri & Navarro-Salas 2005). It follows that the number of elementary particles of type i emitted by the black hole per units of time and energy is

$$\frac{d^2 N_i}{dtdE} = \sum_{dof} \frac{\Gamma_i(E, M)/2\pi}{e^{E/T} \pm 1}, \tag{143}$$

where the sum is taken over the total multiplicity of the particle as well as the angular momentum l of the particle and its projection $m \in \{-l, ..., l\}$ and $\pm$ is for fermions and bosons, respectively. Then, the time-dependent comoving density of Hawking elementary particles i emitted by a distribution of black holes per units of time and energy is

$$\frac{d^2 n_i}{dtdE} = \int_{M_{min}}^{M_{max}} \int_{a^*_{min}}^{a^*_{max}} \frac{d^2 N_i}{dtdE} \cdot \frac{d^2 n}{dMda^*}, \tag{144}$$

where a and a^* are the spin and reduced spin of the black hole defined (see below) for the Kerr case (here set to 0 for a Schwarzschild black hole). The greybody factors describe the probability that a spherical wave representing an elementary particle generated by thermal fluctuations of the vacuum at the black hole horizon escapes its gravitational well. We need to solve the Dirac (spin=1/2) and Proca (integer spin) wave equations for a particle of rest mass μ, i.e.

$$\begin{aligned} (i\not{\partial} - \mu)\psi = 0, \\ (\Box + \mu^2)\phi = 0, \end{aligned} \tag{145}$$

where $\not{\partial} \equiv \gamma^\mu \partial_\mu$ and $\Box = \partial^\mu \partial_\mu$ and use the Schwarzschild metric

$$ds^2 = \frac{1 - r_H}{r} dt^2 - \frac{r}{1 - r_H} dr^2 + r^2 (d\theta^2 + \sin\theta^2 d\phi^2), \tag{146}$$

where $r_H = 2MG$ is the Schwarzschild radius. In these equations, we neglect the couplings between the fields, since they do not affect the probability of emission of (primary) SM particles via Hawking radiation, but they need to be considered in order to obtain the abundance of the final (secondary) particles at infinity, which come from the hadronization/decay of the primary particles. Teukolsky (1972) has shown that the wave equation can be separated into a radial equation and an angular equation if the spherical wave is decomposed into spin-weighted harmonics $S_{sl}(\theta)$ and a radial component $R_s(r)$. For massless particles of spin s, the radial component is

$$\frac{1}{\Delta^s} \frac{d}{dr} \left(\Delta^{s+1} \frac{dR_s}{dr} \right) + \left(\frac{K^2 + is(2r - r_H)K}{\Delta} - 4isEr - \lambda_{sl} \right) R_s = 0, \tag{147}$$

where $\Delta(r) = r(1 - r_H), K(r) = r^2 E^2$ and E is the particle energy (or, equivalently, its frequency). The separation constant $\lambda_{ls} = l(l+1) - s(s+1)$ is the eigenvalue of the angular equation, where l is the angular momentum of the spherical harmonics. Since E must be greater than or equal to μ to emit the particle, the emission spectrum is cut off below $E = \mu$. In order to obtain the greybody factors, we need to compute the transmission coefficients of the wave between the black hole horizon and spatial infinity. These factors depend on the absorption cross-section $\sigma_i(E)$ of the spherical wave on the black hole and it is a sum of all spherical modes l; its behaviour is analogous to the s-dependent diffraction patterns seen in the (true) thermal emission and absorption by a blackbody of a particle whose wavelengths are comparable to the dimensions of the blackbody (MacGibbon & Webber 1990). Thus, we have

$$\Gamma_i(E, M) = \frac{\sigma_i(E, M)E^2}{\pi}. \tag{148}$$

Once the greybody factors are known, it is possible to integrate equation (143) over all energies and sum over all (massive and massless) SM particles to obtain the rate of mass and spin loss of a Schwarzschild black hole through Hawking radiation,

$$\frac{dM}{dt} = -\frac{f(M)}{M^2}, \tag{149}$$

where $f(M)$ is the Page factor obtained by Page (1976) and accounts for the number of quantum degrees of freedom that a black hole of mass M can emit. Its explicit formula is

$$f(M) = -M^2\frac{dM}{dt} = M^2\int_0^\infty \frac{E}{2\pi}\sum_i\sum_{dof}\frac{\Gamma_i(E, M)}{e^{E/T}\pm 1}dE. \tag{150}$$

4.3.2 Kerr Black Holes

If we consider the case of rotating, uncharged black holes with spin $a = J/M$ and reduced spin $a^* = a/M$, where J is the black hole angular momentum, then the temperature is given by

$$T_{\mathrm{Kerr}} = \frac{1}{2\pi}\left(\frac{r_+ - M}{r_+^2 + a^2}\right), \tag{151}$$

where $r_+ = M + \sqrt{M^2 - a^2}$ is the external Kerr radius, then the Dirac and Proca equations (145) have to be developed in the Kerr metric

$$ds^2 = (dt - a\sin^2\theta d\phi)^2\frac{\Delta}{\Sigma} - \left(\frac{dr^2}{\Delta} + d\theta^2\right)\Sigma - \left((r^2 + a^2)d\phi - a dt\right)^2\frac{\sin^2\theta}{\Sigma}, \tag{152}$$

where $\Sigma(r) = r^2 + a^2\cos^2\theta$ and now $\Delta = r^2 - 2Mr + a^2$. The Teukolsky radial equation (147) has to be modified with $K(r) = (r^2 + a^2)E^2 + am$, where m is the projection of angular momentum l. The number of particles of type i emitted per units of time and energy is now

$$\frac{d^2N_i}{dtdE} = \sum_{\mathrm{dof}}\frac{\Gamma_i(E, M, a^*)/2\pi}{e^{E'/T}\pm 1}, \tag{153}$$

where $E' = E - m\Omega$ and $\Omega = a^*/(2r_+)$ is the angular velocity at the horizon. The rotation of the black hole enhances the emission of particles with high angular momentum and with angular momentum projection m aligned with the black hole spin, thus effectively extracting angular momentum from the black hole. We have in this case two Page factors to compute, namely

$$\begin{aligned} f(M, a^*) &= -M^2\frac{dM}{dt} = M^2\int_0^\infty \frac{E}{2\pi}\sum_i\sum_{dof}\frac{\Gamma_i(E, M, a^*)}{e^{E'/T}\pm 1}dE, \\ g(M, a^*) &= -\frac{M}{a^*}\frac{dJ}{dt} = -\frac{M}{a^*}\int_0^\infty \sum_i\sum_{dof}\frac{m}{2\pi}\frac{\Gamma_i(E, M, a^*)}{e^{E'/T}\pm 1}dE. \end{aligned} \tag{154}$$

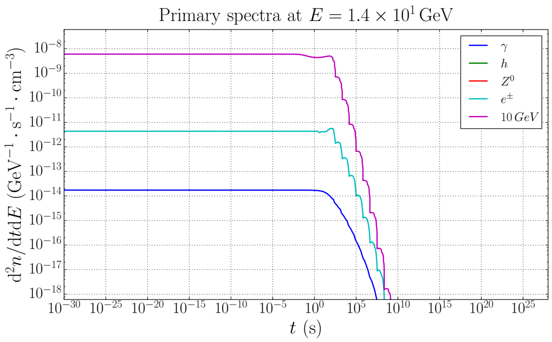

(a)

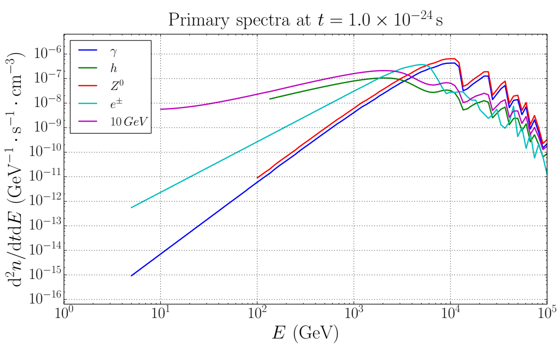

(b)

Figure 8: (a) Kerr Primary Hawking spectra at fixed energy for a 10GeV and 100GeV dark matter particle, respectively. (b) Kerr Primary Hawking spectra at fixed time for a 10GeV and 100GeV dark matter particle, respectively.

.

Using these factors we can also compute the evolution of a^* to be

$$\frac{da^*}{dt} = a^* \frac{2f(M,a^*) - g(M,a^*)}{M^3}. \tag{155}$$

4.4 Results and Discussion

The present purpose of the paper is to calculate the relic abundance of a hypothetical, massive, stable particle species that was in thermal equilibrium in the early Universe. In this paper, we have used the `Blackhawk` code from Arbey & Auffinger (2019) in order to numerically calculate equations (143) and (153) and test some of the assumptions made by Lennon et al. (2018), while assuming that the Hawking decay process starts in a pure pBH-matter-dominated era and $T_{\rm RH} > 3\,\text{MeV}$, the starting temperature of Big Bang Nucleosynthesis. The DM yield also needs to ensure a standard BBN and $\Omega_{DM}h^2 \approx 0.11$ today, as observed.

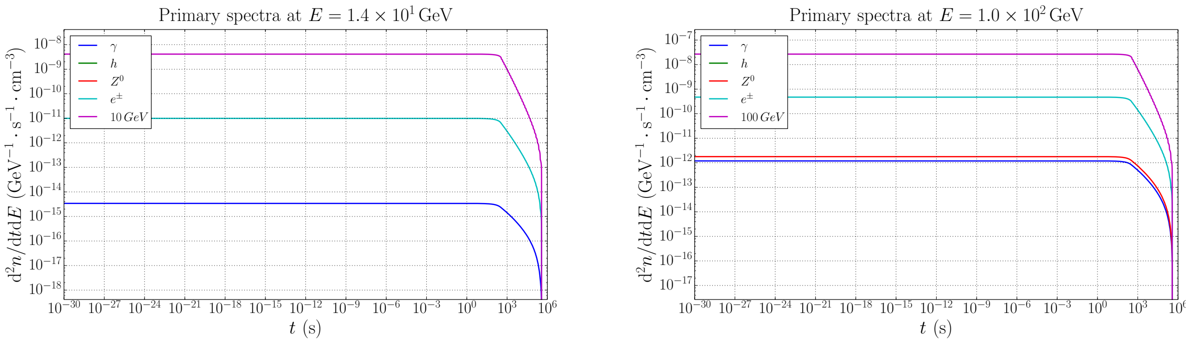

(a)

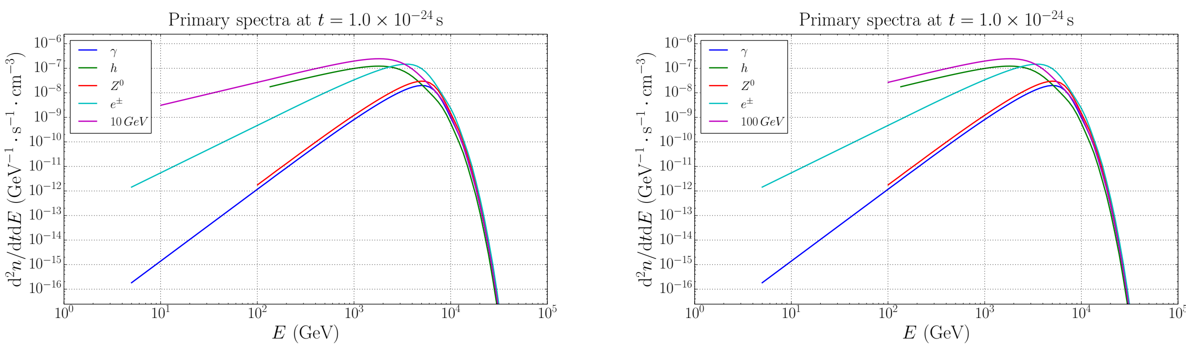

(b)

Figure 9: (a) Schwarzschild Primary Hawking spectra at fixed energy for a 10GeV and 100GeV dark matter particle, respectively. (b) Schwarzschild Primary Hawking spectra at fixed time for a 10GeV and 100GeV dark matter particle, respectively.

We consider that the pBHs have formed in the early universe via the mechanism described in section 4.2.2, which is derived from the scale-invariant model and assumes a power-law power spectrum for the primordial density fluctuations, i.e. equation (132), where $n \approx 1.3$ and $A_{\mathcal{R}_c} = (24.0 \pm 1.2) \times 10^{10}$, as measured from the CMB at the scale $k_0 = 0.002\,\mathrm{Mpc}^{-1}$.

We run simulations for 30 Schwarzschild black holes with masses logarithmically distributed between $M_{\mathrm{min}} = 10^{10}\,\mathrm{g}$ and $M_{\mathrm{max}} = 10^{18}\,\mathrm{g}$ and 30 Kerr black holes with masses logarithmically distributed between $M_{\mathrm{min}} = 10^{10}\,\mathrm{g}$ and $M_{\mathrm{max}} = 10^{18}\,\mathrm{g}$ and spins linearly distributed between $a^* = 0.01$ and $a^* = 0.998$. Note that the spin distribution is independent of the mass distribution. Although there are powerful observational constraints from gravitational microlensing in the subsolar mass regime, a substantial window remains open for pBHs as DM in the mass range extending from the asteroid mass to the mass set by evaporation limits. Depending on the mechanism for production at the end of inflation, there is no restriction on the initial spin of a pBH, up to extremal values $a^* \approx 1$ (Arbey et al. 2020). We take the maximum spin to be $a^* = 0.998$, the Thorne limit for BHs with astrophysical origin. This limit comes from accretion of the surrounding gas on a BH and its balance with superradiance effects. The primary Hawking spectra obtained are given in figures 8 and 9 for a simulated DM particle with $E = 10$ GeV, 2 dof and spin 0 and a DM particle with $E = 100\,\mathrm{GeV}$, 2 dof and spin 0; the plots can be compared to those obtained by Arbey et al. (2020) and Carr et al. (2010). These confirm the claim made by Lennon et al. (2018) that the monochromatic BH spectrum can be extended to a broader mass distribution without affecting the final results.

The `Blackhawk` code uses routines that compute the comoving densities $dn(M, a^*)$, where dM is taken around the considered mass and da^* around the considered spin and then rescales the results by a factor 10^{100}, due to the very small numbers involved. The black hole initial masses, spins and comoving densities are written in a text file, then the Euler method is used to compute the loss rates of each of the BH masses and BH spins. The greybody factors are used in order to compute the emissivity $d^2n/dtdE$; the output is tabulated in a text file containing on the first line a list of energies (in GeV), on the first column a list of times (in s) and each further column is the emission rate of the particle per unit energy, time and covolume. To fit the present purpose, all source code routines (e.g. the greybody and Page factors) had to be modified and recomputed in order to account for a new primary (DM) particle, and additional variables have been defined within the code to specify the particle spin and number of degrees of freedom. Additionally, all the new particles have been added to the fixed length arrays of particle types. In order to obtain the comoving number density of dark matter particles from the file output, we have used the trapeze numerical rule to integrate over all times and all energies. The results are given in Appendix A below and need to also be rescaled by a factor of 10^{100}.

4.5 Summary and Future Work

In summary, we have numerically analyzed the black holes and spectra evolution by considering the energy and angular momentum losses via Hawking radiation. The present application is to study the effects of primary dark matter particles generated by a distribution of pBHs on observable quantities. A new feature introduced in this paper is the ability of the code to also test the effects of a black hole spin distribution on the particle yield. An analysis and comparison of the dark matter yield results with those in Lennon et al. (2018) will be made in a future work. These have the potential of reducing a wide range of parameter space for current and future cosmological models that imply dark matter formation, as well as to test Hawking radiation assumptions and study black hole properties.

The elementary particles emitted by BHs are not the final products of the Hawking emission; some of them are unstable, and others only exist in hadrons. The spectrum of injected particles will therefore have two components: a primary component which creates a particle directly and a secondary component made from the decay and hadronization of the primary component. We can further use the `HERWIG` and `PYTHIA` codes within `Blackhawk` in order to obtain the secondary Hawking emission - this depends on the cosmological context in which it is emitted. These results will be further compared with the ones given by MacGibbon & Webber (1990)).

5 Conclusions

In this paper, we have explicitly calculated the Hawking result and presented a proposal to address the black hole information paradox that modifies QM unitary evolutions. Although several simplifying assumptions have been made, such as the reliance on semiclassical gravity, or ignoring the backreaction effects, the purpose of implementing the CSL model for a two-dimensional black hole metric considered here was to outline the basic features that a fully four-dimensional covariant setting should include.

Moreover, this paper's aim was to consider a realistic evaporation framework, where backscattering modifies the emission of particles. This idea was applied numerically in the context of black holes formed by collapse of primordial inhomogeneities, in order to test the allowed ranges for the dark matter yield, and consequently to constrain possible early Universe scenarios.

A Blackhawk results

```
Kerr Primary Hawking Flux - Dark Matter particle with E=100GeV, spin=0, dof=2
Reading primary spectrum file for particle dark
Time for reading file is 18.0493781567 seconds
Computing total flux for particle dark with trapezoidal method
Energy interval: [0.0005,41000.0] GeV
Time   interval: [1e-30,4.84898e+27] seconds
Total flux of particle dark is 0.9507711140183361

Kerr Primary Hawking Flux - Dark Matter particle with E=10GeV, spin=0, dof=2
Reading primary spectrum file for particle dark
Time for reading file is 18.3895449638 seconds
Computing total flux for particle dark with trapezoidal method
Energy interval: [0.0005,41000.0] GeV
Time   interval: [1e-30,4.84898e+27] seconds
Total flux of particle dark is 0.9520306413790577

Schwarzschild Primary Hawking Flux - Dark Matter particle with E=100GeV, spin=0, dof=2
Reading primary spectrum file for particle dark
Time for reading file is 3.59689497948 seconds
Computing total flux for particle dark with trapezoidal method
Energy interval: [0.0005,41000.0] GeV
Time   interval: [1e-30,5.57591e+27] seconds
Total flux of particle dark is 1.6419446321543603

Primary Schwarzschild Hawking Flux - Dark Matter particle with E=10GeV, spin=0, dof=2
Reading primary spectrum file for particle dark
Time for reading file is 3.67286801338 seconds
Computing total flux for particle dark with trapezoidal method
Energy interval: [0.0005,41000.0] GeV
Time   interval: [1e-30,5.57591e+27] seconds
Total flux of particle dark is 1.6446448527442747
```

B A meme

This section has been created to honour one of the pillars of my physics degree - memes. .

References

1. Arbey A., Auffinger J., 2019, The European Physical Journal C, 79
2. Arbey A., Mahmoudi F., 2021, Progress in Particle and Nuclear Physics, 119, 103865
3. Arbey A., Auffinger J., Silk J., 2020, Monthly Notices of the Royal Astronomical Society, 494, 1257–1262
4. Battaglieri M., et al., 2017, US Cosmic Visions: New Ideas in Dark Matter 2017: Community Report (arXiv:1707.04591)
5. Bedingham D. J., 2010, Foundations of Physics, 41, 686–704
6. Bedingham D., Modak S. K., Sudarsky D., 2016, Physical Review D, 94
7. Carr B. J., Kohri K., Sendouda Y., Yokoyama J., 2010, Physical Review D, 81
8. Cowan B., 2005
9. Fabbri A., Navarro-Salas J., 2005
10. Giddings S. B., Nelson W. M., 1992, Physical Review D, 46, 2486–2496
11. Green A. M., Liddle A. R., Malik K. A., Sasaki M., 2004, Physical Review D, 70
12. Hawking S., 1971, Mon. Not. Roy. Astron. Soc., 152, 75
13. Hawking S. W., 1975, Commun. Math. Phys., 43, 199
14. Hossenfelder S., Smolin L., 2010, Physical Review D, 81
15. Kolb E. W., Turner M. S., 1990, The Early Universe. Vol. 69
16. Lennon O., March-Russell J., Petrossian-Byrne R., Tillim H., 2018, JCAP, 04, 009
17. MacGibbon J. H., Webber B. R., 1990, Phys. Rev. D, 41, 3052
18. Masina I., 2021, Dark matter and dark radiation from evaporating Kerr primordial black holes (arXiv:2103.13825)
19. Mathur S. D., 2009, Classical and Quantum Gravity, 26, 224001
20. Modak S. K., Ortíz L., Peña I., Sudarsky D., 2015, General Relativity and Gravitation, 47
21. Mukhanov V., Winitzki S., 2007, Introduction to Quantum Effects in Gravity. Cambridge University Press, doi:10.1017/CBO9780511809149
22. Okon E., Sudarsky D., 2014, Foundations of Physics, 44, 114–143

23. Page D. N., 1976, Physical Review D, 13, 198

24. Penrose R., 2004, The Road to Reality: A Complete Guide to the Laws of the Universe

25. Pontzen A., Peiris H., 2020

26. Shibata M., Sasaki M., 1999, Physical Review D, 60

27. Teukolsky S. A., 1972, Phys. Rev. Lett., 29, 1114

28. Tomonaga S., 1946, Progress of Theoretical Physics, 1, 27

29. Wald R. M., 1984, General Relativity. Chicago Univ. Pr., Chicago, USA, doi:10.7208/chicago/9780226870373.001.0001